Journal of Integrative Neuroscience

J. Integr. Neurosci. **2026**; 25(11): 50889
https://doi.org/10.31083/JIN50889

Original Research

Nasal Respiratory Training Induces Neuromorphological Changes in Hippocampus and Default Mode Network Structures Accompanied by Reduced Physiological Stress Parameters — A Randomized MRI Trial

Alexej Silenko[1], Tabea Reckner[1], Ronja Hübner[1], Christoph Krick[1,*], Wolfgang Reith[1,*]

[1]Department for Neuroradiology, Medical Faculty, Saarland University, D-66424 Homburg, Germany
*Correspondence: christoph.krick@uks.eu (Christoph Krick); wolfgang.reith@uks.eu (Wolfgang Reith)
Academic Editors: Changjong Moon and Bettina Platt
Submitted: 10 February 2026 Revised: 8 August 2026 Accepted: 21 August 2026 Published: 12 November 2026

Abstract

Background: Conscious nasal breathing (*pranayama*) is essential to the beneficial effects of yogic mind-body interventions on brain health and neurovegetative stress mitigation. In the present voxel-based morphometry (VBM) study, we sought to explore the relationship between physiological stress parameters and structural central nervous system (CNS) changes as a result of daily nasal *pranayama* training. **Methods:** A total of 101 young healthy yoga novices were randomized into a nasal intervention group (N), an oral control group (M), and a passive control group (C). For 4 weeks, the nasal and oral groups performed the same daily sequence of respiratory exercises through the nose and mouth respectively. In addition to heart rate (HR), blood pressure (BP), and salivary cortisol level (sCort) measurements, multiple periodic structural (sMRI) and functional (fMRI) magnetic resonance imaging scans were acquired for each participant. Structural MRI data were analyzed via voxel-based morphometry. A detailed analysis of functional MRI data was performed in a separate study. **Results:** Two and four weeks of daily nasal *pranayama* stimulated significant gray matter (GM) density changes within limbic structures, such as the left posterior hippocampus (HC) and medial prefrontal cortex (mPFC). GM density increases in default mode network (DMN) structures, such as the hippocampus and precuneus, were predicted by fMRI as well as lower mean salivary cortisol and lower mean heart rate in the nasal intervention group. Oral respiratory training led to scattered GM density growth primarily in the right amygdala and bilateral insulae without a significant association with fMRI data or physiological stress parameters. **Conclusions:** Daily nasal *pranayama* training leads to significant structural sMRI effects in stress-sensitive brain regions. The neuroanatomical distribution pattern of these sMRI findings is distinct from observations in the oral control group. Only the structural effects in the nasal intervention group are consistent with and predicted by fMRI and concomitant changes in physiological stress markers. **Clinical Trial Registration:** DRKS00039396. Registered 26 February, 2026, https://www.drks.de/search/en/trial/DRKS00039396/details. (This study was retrospectively registered via the German Clinical Trials Register with all due transparency regarding data, methodology, and underlying administrative delays in the registration).

Keywords: yoga; breathing; pranayama; stress; structural neuroplasticity; voxel-based morphometry; MRI; hippocampal formation

1. Introduction

Breath control (*pranayama*) has been a cornerstone of yogic tradition for millennia. Amongst other elements of yoga, like physical postures (asanas) and meditation (dhyana), nasal respiratory exercises improve general well-being [1,2], cardiovascular [3,4,5], respiratory [6], and neuropsychiatric health [7]. In large part, these effects can be attributed to a multilevel modulation of the stress response, including central nervous, peripheral neurovegetative, and neurohumoral pathways [8]. To our knowledge, the specific impact of nasal *pranayama* on structural central nervous system (CNS) plasticity in relation to peripheral surrogates of the stress response has not been examined yet.

However, a growing body of literature demonstrates structural magnetic resonance imaging (MRI) changes for holistic yoga approaches [9,10,11] and comparable mind-body interventions (MBI), featuring elements of meditation, mindfulness, and physical activity [12,13,14]. These findings predominantly concentrate on stress-sensitive brain regions involved in higher-order self-referential cognitive and emotional processing, such as the medial prefrontal cortex and hippocampal formation. Functional MRI and electroencephalography (EEG) studies likewise reaffirm the importance of these neuroanatomical foci in the context of Default Mode Network (DMN) [15] modulation through MBI [16,17].

As a major caveat, most studies do not differentiate between the various elements of their respective intervention paradigms and cannot attribute their significant MRI effects to specific components, e.g., nasal *pranayama* as a key element of yoga. This problem is further complicated by the intricate synergistic relationship between interoceptive elements, such as meditation and conscious breathing [18].

Aware of these challenges, our research group set out to explore the specific element of nasal *pranayama* after performing a successful functional magnetic resonance

Copyright: © 2026 The Author(s). Published by IMR Press.
This is an open access article under the CC BY 4.0 license.

Publisher's Note: IMR Press stays neutral with regard to jurisdictional claims in published maps and institutional affiliations.

imaging (fMRI) pilot study [M. Garner & C. Krick, personal communication, 2020] showing hippocampal activation through nasal, not oral, breathing, similar to previous findings by Jung et al. [19]. We chose a combined explorative fMRI and structural magnetic resonance imaging (sMRI) approach to investigate whether such short-term differences in activation could be reproduced and translated into sustained structural MRI differences through four weeks of daily nasal vs oral *pranayama*. Additionally, we tracked physiological stress parameters, such as heart rate, blood pressure, and salivary cortisol levels, in order to study the relationship between central neural and peripheral vegetative predictors of *pranayama*-induced stress reduction, and to monitor for potential adverse effects of the respiratory and imaging procedures.

2. Materials and Methods

2.1 Study Design

For this longitudinal, controlled, randomized, interventional MRI study, a total of 101 healthy individuals were recruited by means of local and digital advertisement. Building on previous voxel-based morphometry (VBM) yoga studies in our department [20], a minimum sample size equal to or greater than 100 was determined as sufficiently powered for this approach. An a priori power analysis for a repeated-measures ANOVA (within-between interaction) targeting structural gray matter density change as the primary outcome yielded a required sample of N = 90 ($f = 0.25$, $\alpha = 0.001$, $1 - \beta = 0.95$, $\rho = 0.5$). The expected effect size was conservatively estimated at one-quarter of the large functional effect observed in our pilot fMRI study ($d \approx 1.0$; 95% CI [0.72, 1.35], $p < 0.001$), reflecting the lower anticipated magnitude of structural neuroplasticity relative to acute functional activation. The final enrolled sample (N = 101) incorporated an estimated ~12% attrition allowance. No interim analyses or stopping guidelines were prespecified; the trial was conducted to its planned completion. The sample's mean age was 26.78 years (± SD 8.52 years; range: 18 to 62 years). Subjects included were over the age of 18, self-reported to be healthy with no history of relevant neuropsychiatric, cardiovascular, or bronchopulmonary disease and abstaining from psychoactive substances. Explicitly excluded were bearers of MRI-incompatible implants, epileptic patients as well as those affected by insurmountable claustrophobia.

To optimize the signal-to-noise ratio we set a four-week intervention period [21] with a pre-, post-, and mid-test point of measurement at the two-week mark. The sample was organized into three groups: oral control group M (n = 28), passive control group C (n = 34), nasal intervention group N (n = 39). This allowed us to specify the neurostructural effects of the respiratory training and to mitigate the impact of potential external and internal confounders. A random number generator assigned active participants to their respective group. Simple randomisation without blocking or stratification was used. The allocation sequence was generated prior to enrolment and concealed in sealed notebooks until assignment. The enrolling researcher had no access to the sequence until after participant enrolment. Study subjects received no information about the study's hypotheses prior to inception except for the general design and the existence of active and non-active groups. MRI data were acquired by independent technical assistants and transferred to automated processing in an anonymized number format. However, complete double blinding was not possible in view of information ethics regarding incidental MRI findings, in which case we were required to be able to trace back the anonymized data files to individual participants as per ethics commission guidelines.

Both groups executed a daily 20-minute-long sequence of *pranayama*-based breathing exercises throughout the four-week intervention period, either orally (M) or nasally (N). Subjects from both groups were asked to confirm their lack of prior experience in the field of yogic breathing techniques and the absence of extreme changes to their physical or recreational activities in the preceding six months. The passive control group did not change their normal routine and habits.

In order to ensure repeatability and practicality, data were collected in two acquisition intervals, resulting in two cohorts (May 2021–August 2021, n = 52; November 2021–May 2022, n = 49) following an identical study design. For the final analysis, data from both cohorts were unified in one data sheet.

All subjects participated voluntarily and signed an informed consent document. Participation was compensated with a copy image of the MRI brain scan in addition to either 25 euros (group C) or 50 euros (groups N and M).

Data acquisition methods used in this study comprised structural cranial magnetic resonance imaging (cMRI) scans, salivary cortisol samples, oscillometric blood pressure and heart rate measurements. Functional MRI scans were also performed and will be referenced in this work, while the detailed presentation and discussion of our extensive fMRI results will be the subject of a separate work.

No patients or members of the public were involved in the design, conduct, or reporting of this trial.

2.2 Intervention

Both the nasal intervention group and the oral control group executed a 20-minute-long sequence of *pranayama*-based respiratory exercises every day for a total of four weeks (see Fig. 1).

The respiratory sequence (see Fig. 2) was developed in consultation with a researcher from our department, who had received formal training in Hatha Yoga at SVYASA Yoga University. It was composed of two parts:

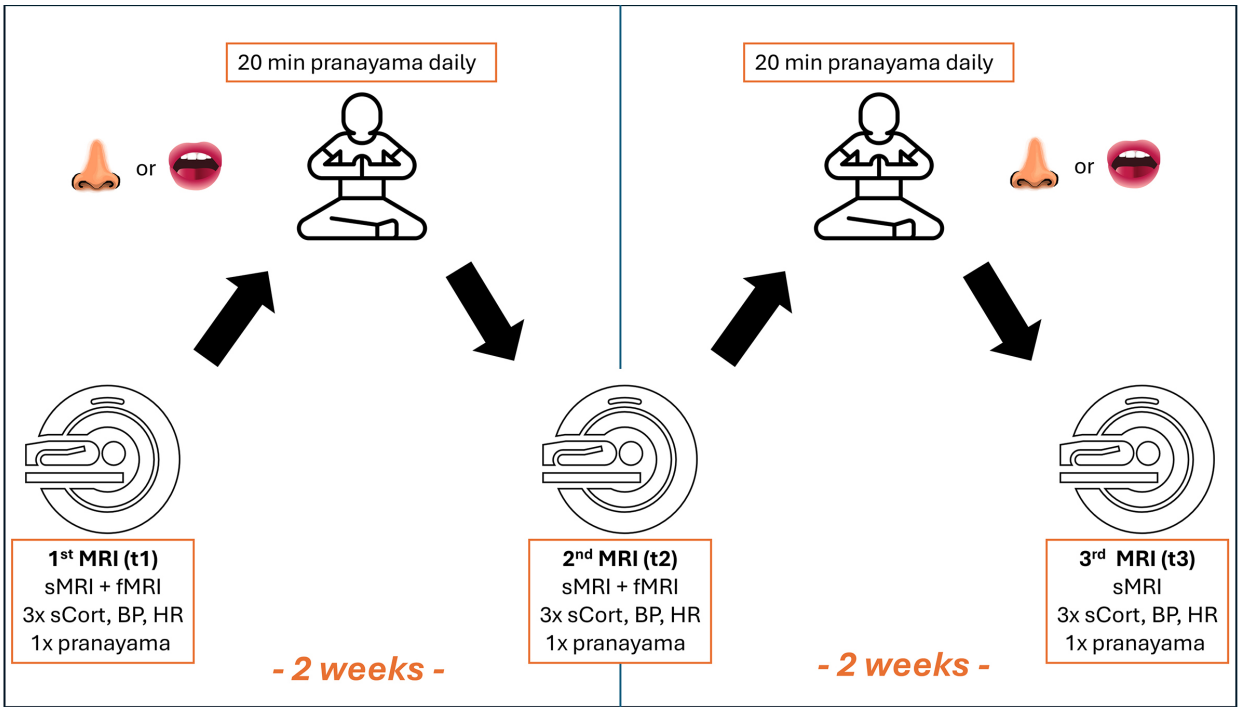


Fig. 1. Schematic overview of the general study design including three appointments in the MRI laboratory and daily breathing exercises (*pranayama*) at home. sCort, salivary cortisol level; BP, blood pressure; HR, heart rate; sMRI, structural magnetic resonance imaging; fMRI, functional magnetic resonance imaging.

- a 60-second-long segment of controlled deep hyperventilation (~60 breaths per minute) with passive inspiration and forced expiration *(vatakrama kapalbhati)*,
- followed by a 19-minute-long segment of controlled deep hypoventilation (≤3 breaths per minute) involving abdomen, diaphragm, and chest *(dirgha pranayama)*.

During the hypoventilation segment, expirations and inspirations were separated by seconds-long voluntarily controlled breath retention intervals (kumbhaka).

The intervention was mostly conducted in the domestic environment, except for the study's three measurement appointments at our MRI facility. Here, the participants were meticulously instructed, corrected, if need be, and introduced to a self-designed website with instructive videos intended to assist them in maintaining the correct frequency, amplitude, and technique at home. By virtue of being complete novices, our subjects could not be expected to immediately reach the target frequency and duration. Therefore, the website featured a levelling system enabling the overwhelming majority to reach the exact target in a couple of days (see Fig. 3). Success and progress were likewise self-documented by means of a supplied diary template.

Additionally, the first and second measurement appointments featured an fMRI experiment (26.67 minutes) involving four repeating cycles of nasal and oral breathing conditions. One cycle was always structured in the following way:

1. 20 seconds of fast nasal breathing (60 breaths per minute).
2. 120 seconds of slow nasal breathing (3 breaths per minute).
3. 60 seconds of normal-frequency breathing (14 breaths per minute) + blood pressure measurement.
4. 20 seconds of fast oral breathing (60 breaths per minute).
5. 120 seconds of slow oral breathing (3 breaths per minute).
6. 60 seconds of normal-frequency breathing (14 breaths per minute) + blood pressure measurement.

During the fMRI experiment, visual cues guided the participants' respiratory pacing and airway route: A dynamically rising and sinking animated bar regulated the respiratory rate, while an image of either a nose or a mouth indicated the required breathing orifice. Oscillometric blood pressure measurements were accompanied by the presentation of an additional blood pressure device icon.

2.3 Data Acquisition

A total of three T1-weighted structural cMRI scans were acquired in four weeks by means of a 3.0 Tesla MRI scanner (Magnetom Skyra, Siemens, Erlangen, Germany, syngo MR E11) equipped with a 20-channel head array coil: the first one at the study's inception (t1), the second one after two weeks (t2), and the third one after four weeks (t3). During the respective scans, high-resolution, whole-brain images were collected as well as a T1-weighted Magnetiza-

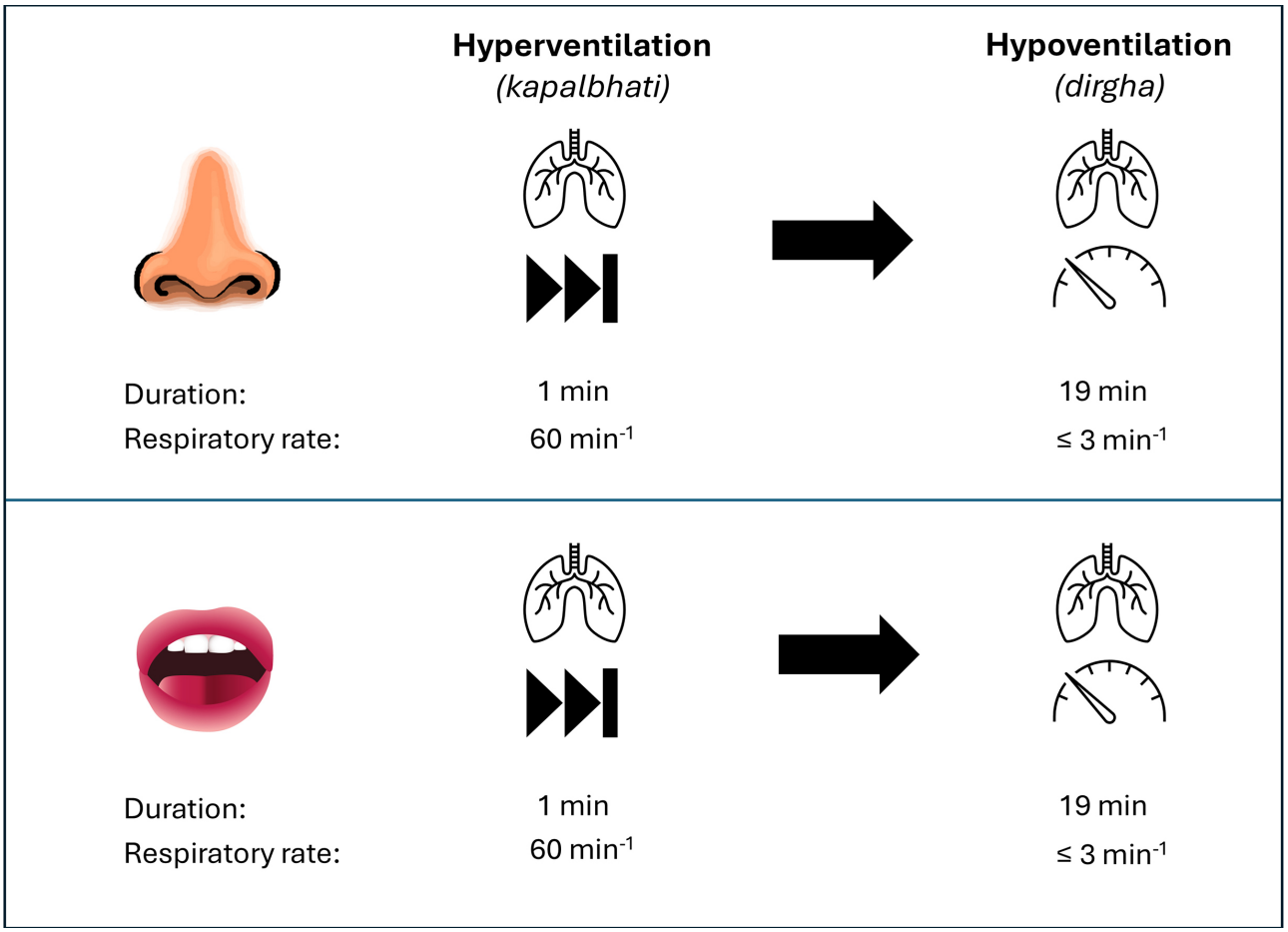


Fig. 2. Schematic overview of respiratory sequence comprising a short high-amplitude hyperventilation segment (kapalbhati) and a long high-amplitude hypoventilation segment (dirgha).

tion Prepared Rapid Gradient Echo (MPRAGE) sequence, comprising 192 sagittal slices (Matrix: 256 × 256 pixels; inversion time (TI) = 900 ms; echo time (TE) = 2.13 ms; repetition time (TR) = 1900 ms; Flip angle = 9°; field of view (FoV) = 240 mm; slice spacing and thickness = 0.9 mm).

Structural cMRI scans were preceded by the acquisition of T2*-weighted, whole-brain functional cMRI scans on the first and second measurement appointment. We used gradient-echo echo-planar imaging (EPI) sequence with the following parameters: TR = 3.5 s; TE = 30 ms; flip angle = 90°; 49 axial slices; matrix size = 94 × 94; slice thickness = 1.43 mm; slice gap = 0.5 mm; FOV = 134 × 134 mm; and voxel size = 2 × 2 × 2 mm^3.

The acquired MRI data were then pre-processed according to the voxel-based morphometry method (VBM) in CAT 12 (Computational Anatomy Toolbox, 12.8.1 [r1975], Jena, Germany, https://neuro-jena.github.io/cat12-help/, [22]) and the MATLAB-based (MathWorks, Inc., R2021a & R2021b, Natick, MA, USA) software package SPM 12 (Statistical Parametric Mapping, r7487 & r7771, Wellcome Centre for Integrative Neuroimaging, UCL, London, UK, https://www.fil.ion.ucl.ac.uk/spm/).

Voxel-based morphometry is a well-established statistical brain modelling method based on voxel-wise comparison of local GM and/or WM tissue concentration gradients [23,24]. It allowed us to systematically examine structural whole-brain effects and group differences with a high regional specificity [25]. To this end, MRI images were subjected to three pre-processing steps, the first two of which were executed in CAT 12. First, the images were segmented into gray matter (GM), white matter (WM) and cerebrospinal fluid (CSF) through a more precise and refined segmentation process [22], as compared to the standard SPM 12 Unified Segmentation approach [26]. Subsequently, the images were normalized and registered to the same stereotactic space. This is achieved through a DARTEL algorithm generated template (Diffeomorphic Anatomical Registration Through Exponentiated Lie Algebra) [27,28], which is embedded in an MNI coordinate system (Montreal Neurological Institute) and based on 555 healthy control subjects of the IXI-database (http://brain-development.org/ixi-dataset/). Different linear and non-linear transformations enabled the images' coordinates to be compared and adapted to the template with a reference point in the anterior commissure. Transformation factors

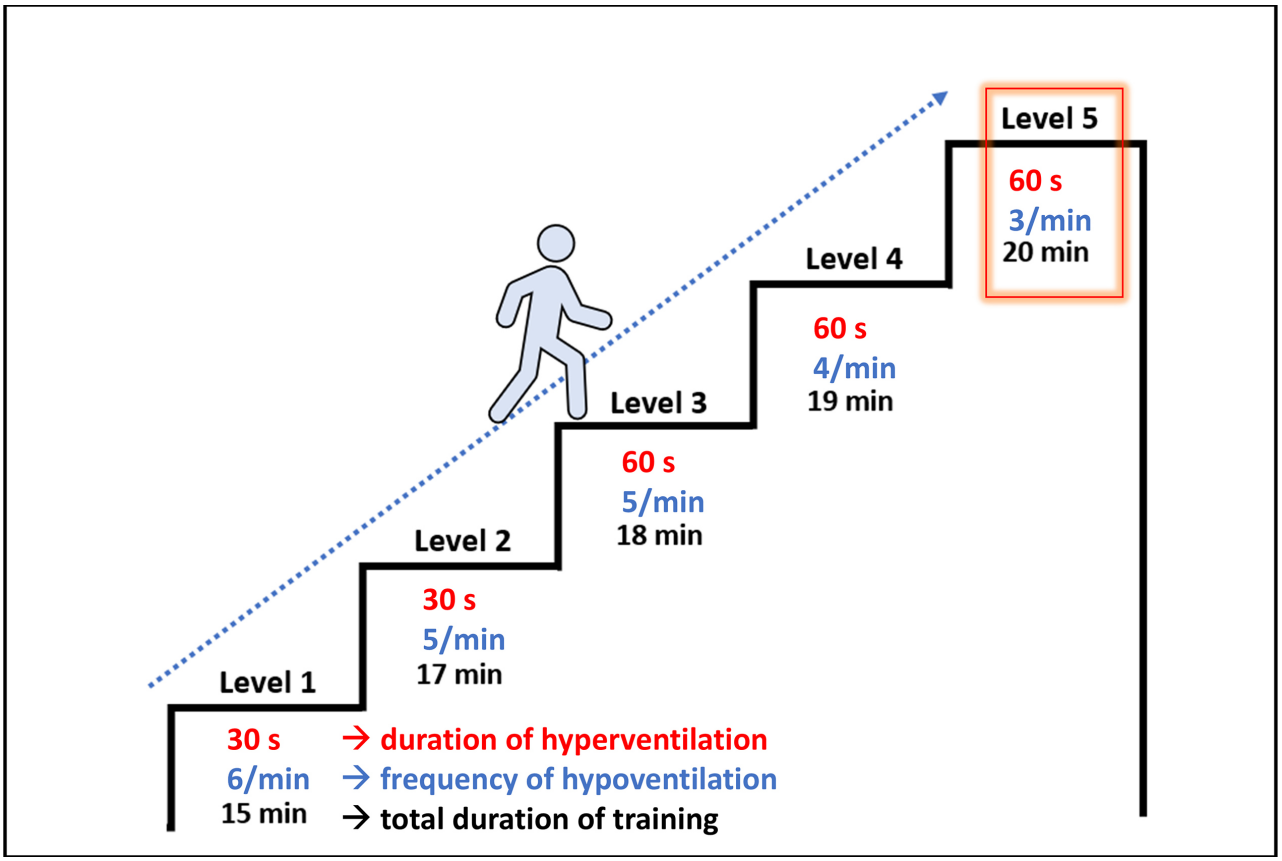


Fig. 3. Schematic overview of gradual levelling system for our *pranayama* novices. Participants were encouraged to reach level 5 (our target) within the first week and document progress in a diary provided by us. Except for few exceptions, everyone reached the target in the intended time frame.

were registered in a Jacobian matrix and its resulting determinant permitted later retrograde calculation. The final processing step was carried out in SPM 12 and involved Gaussian smoothing with a 10-mm Full Width at Half Maximum (FWHM) Gaussian kernel to reduce noise [29]. The local distribution of the three compartments (GM, WM, CSF) was not affected by this process, nor were the tissue density values represented by the respective local concentration gradients.

For pre-processed unmodulated VBM data, changes in the proportion of gray matter relative to other tissues within a given brain region can then be interchangeably described as gray matter concentration or density changes [30]. In this paper, we exclusively use the term "gray matter density" to refer to the same concept.

Three physiological stress parameters were measured at pretest (t1), midtest (t2), and posttest (t3) points, before and after *pranayama* exercise. These included the measurement of heart rate and blood pressure via digital sphygmomanometer (model UA-651SL; standard adult arm cuff, circumference 23–37 cm; A&D Company, Limited, Toshima, Tokyo, Japan; https://www.admedical.com) as well as salivary cortisol samples via Salivette® saliva collection device (art. no. 51.1534.500; Sarstedt AG & Co. KG, Nümbrecht, North Rhine-Westphalia, Germany). All three measurement appointments were rigorously scheduled and coordinated with the subjects in such a way as to ensure that physiological stress parameters, especially salivary cortisol samples, were always acquired at the same time of day, exactly two weeks after the previous sample. Storage, analytic capacity, quality control, and supervision in this matter were provided by the Central Laboratory of the Saarland University Hospital.

A standard protocol for a given measurement day therefore included the following steps:

1. Arrival and registration of participant followed by 5–10 minutes of seated waiting in a low stimulation environment.
2. First round of physiological stress data acquisition: blood pressure, heart rate, salivary cortisol levels (5 minutes).
3. Functional and structural MRI scan acquisition in the room immediately adjacent to the initial registration room (30 minutes).
4. Second round of physiological stress data acquisition in the registration room: blood pressure, heart rate, salivary cortisol levels (5 minutes).

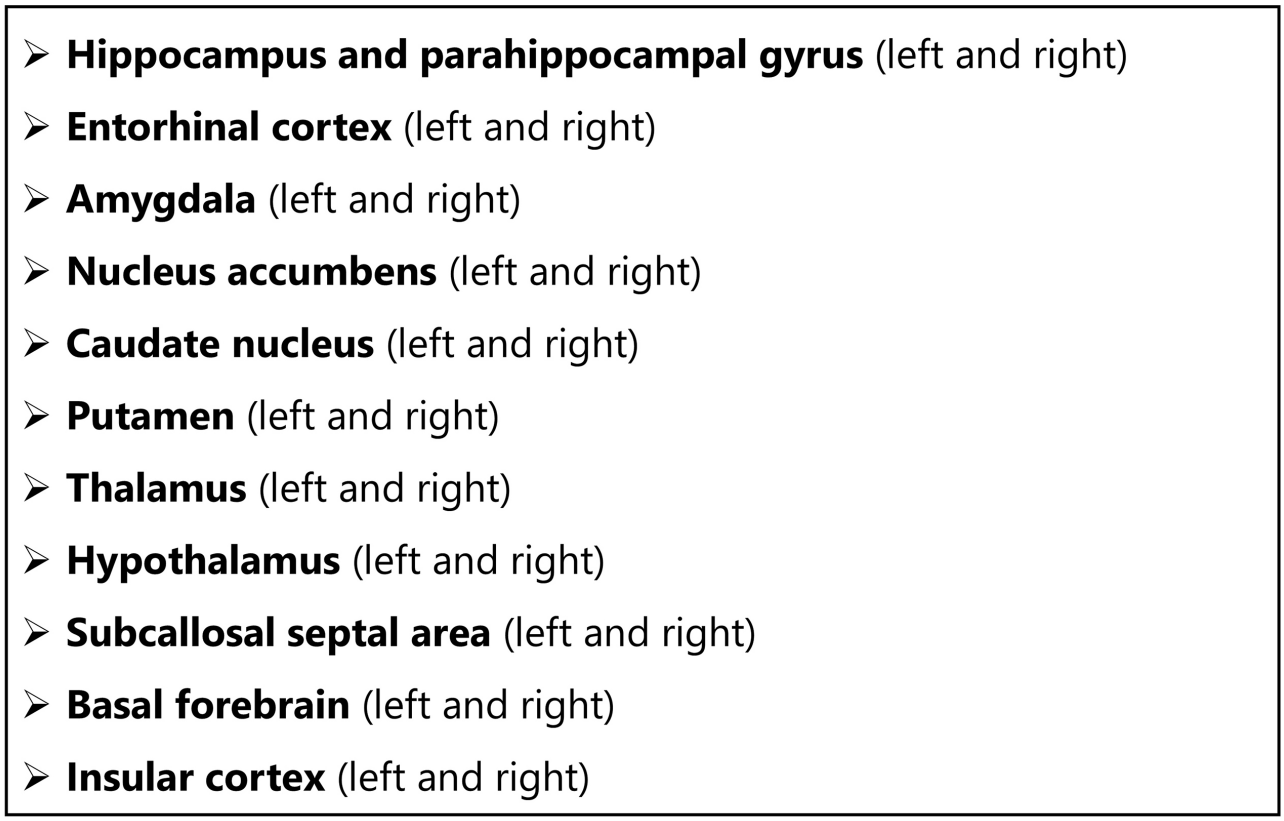


Fig. 4. List of neuroanatomical structures included in post hoc mask for group comparison analysis as regions of interest (ROI).

5. Supervised execution of respiratory sequence orally or nasally outside the registration room, depending on active group membership, or no respiratory intervention and same duration of seated waiting in the passive control group (15–20 minutes).
6. Third round of physiological stress data acquisition outside the registration room while subjects remained motionlessly seated: blood pressure, heart rate, salivary cortisol levels (5 minutes).

2.4 Statistical Processing

After pre-processing, the MRI datasets were analyzed in an SPM12-designed flexible factorial model contrasting group-specific structural GM changes across the three groups (N, M, C) within the framework of the General Linear Model. In accordance with our anatomical hypotheses, preceding studies [20], and available literature [31,32,33,34], we designed a post-hoc mask via CAT12-distributed Neuromorphometrics probabilistic atlas (Neuromorphometrics, Inc., 20131115, South Bend, IN, USA; https://www.neuromorphometrics.com) with several regions of interest (ROIs) for the rendering of group comparison results (see Fig. 4). Thus, we significantly limited the number of multiple comparisons and set the significance level to uncorrected $p < 0.05$ for our longitudinal data and cluster extent threshold of 20 voxel.

Functional MRI results were analyzed in a separate work with the significance level set to Family-Wise Error (FWE) corrected $p < 0.05$.

In addition to the abovementioned flexible factorial model, we constructed a paired whole-brain multiple regression model within the framework of the General Linear Model, separately featuring the three physiological stress parameters as independent regressors (covariates) in order to determine which brain regions underwent structural change (uncorrected $p < 0.001$; cluster extent threshold = 20 voxel) in relation to *pranayama*-mediated autonomic stress effects.

For further statistical processing, significant clusters were extracted and transferred to a common IBM SPSS Statistics, version 27.0 (IBM Corp., Armonk, NY, USA; https://www.ibm.com/products/spss-statistics) data sheet, comprising all types of data and parameters collected in the study.

The Shapiro–Wilk test flagged detectable departures from normality for most parameters (e.g., change in mean heart rate, t2–t1: W = 0.961, n = 97, $p = 0.005$). Given the sensitivity of this test at this sample size, a conservative nonparametric approach was adopted throughout.

Significance levels for all pairwise comparisons were stringently corrected using the Bonferroni procedure.

Aware of the strictly associative nature of regression analyses, we report the results as per convention in terms of significant predictors and response variables without claiming directionality or causality.

2.5 Harms and Safety Monitoring

Harms were assessed systematically rather than incidentally. At each of the three measurement appointments (t1, t2, t3), all participants were directly queried about any adverse symptoms associated with the respiratory intervention, with particular attention to events linked to the controlled hyperventilation segment (kapalbhati), including dizziness, light-headedness, presyncope, dyspnoea, and subjective discomfort. MRI-related safety was ensured a priori through strict enforcement of the exclusion criteria and through continuous supervision during scan acquisition. Any reported symptom was to be documented and attributed to either the intervention, the imaging procedure, or an unrelated cause.

This trial is reported in accordance with the CONSORT 2025 guideline for randomised trials; the completed CONSORT 2025 checklist is provided as **Supplementary Material**.

3. Results

3.1 Sociodemographic Profile and Compliance

Out of the initial 101 subjects present at the pretest measurement appointment (t1), 97 attended the midtest appointment (t2) two weeks later, and 81 attended the final posttest measurement appointment (t3) after the completion of the four-week training period.

The overall compliance of 88.66 ± 16.93% based on *pranayama* diary data was rated as sufficiently high. The few incompliant outliers were still included in accordance with an intention-to-treat approach. Among these outliers were the only 3 participants who took more than 3 days to reach level 5 (see Fig. 3), while the majority of the sample did so in 1–3 days. 74.4% of individuals reported performing *pranayama* in the late day hours, 4 pm–12 am.

Despite a higher total number of women partaking in the study (71 women vs 30 men), no significant relation between gender and assigned group could be found in a chi-square test of independence (χ^2 (2) = 2.766; p = 0.251). Age had no significant relation to assigned group either (independent-samples Kruskal-Wallis test: H = 0.860; df = 2; p = 0.650), averaging at 26.78 years (±SD 8.52 years; range: 18 to 62 years).

3.2 Physiological Stress Parameters

As far as pretest baseline values are concerned, none of the three types of physiological stress parameters differed significantly across groups, except for the mean pretest diastolic blood pressure value (independent-samples Kruskal-Wallis test: H = 8.027; df = 2; p = 0.018), with pairwise comparison primarily revealing a significantly higher base value for the nasal intervention group N as compared to the passive control group C (Bonferroni adjusted p = 0.019; z = –2.734).

However, it should be noted that the mean diastolic pressure of the passive control group did not evolve across the four weeks, whereas the nasal intervention group N and oral control group M did show a significant decrease in the first two weeks [t2–t1, Wilcoxon Signed Ranks test: p (N) = 0.001; Z = –3.184 vs p (M) = 0.019; Z = –2.355 vs p (C) = 0.141; Z = –1.471] and the entire four weeks [t3–t1, Wilcoxon Signed Ranks test: p (N) = 0.008; Z = –2.665 vs p (M) = 0.008; Z = –2.651 vs p (C) = 0.133; Z = –1.503]. Systolic blood pressure presented no such dynamic, remaining stable across groups.

The mean heart rate of the nasal intervention group N saw a highly significant decrease in the first two-week period in contrast to the other two groups [t2–t1, Wilcoxon Signed Ranks test: p (N) = 0.001; Z = –3.300 vs p (M) = 0.060; Z = –1.880 vs p (C) = 0.830; Z = –0.215]. In turn, the last two weeks resulted in all three groups' mean heart rates rising, although the nasal intervention group N and oral control group M remained below their pretest base values. Only the nasal intervention group N had a significantly lower mean heart rate than the passive control group C (Bonferroni adjusted p = 0.045; z = 2.429).

Mean salivary cortisol levels (sCort) mirrored the mean heart rate, falling significantly in the intervention group N within the first two weeks [t2–t1, Wilcoxon Signed Ranks test: p (N) = 0.011; Z = –2.577 vs p (M) = 0.209; Z = –1.257 vs p (C) = 0.746; Z = –0.323]. The intervention group's t2 sCort base value was significantly lower than its t1 value, especially in comparison to the passive control group (Bonferroni adjusted p = 0.020; z = 2.710).

Mean sCort uniformly increased in all three groups during the last two weeks [t3–t2, Wilcoxon Signed Ranks test: p (N) = 0.001; Z = –3.315 vs p (M) = 0.021; Z = –2.301 vs p (C) = 0.001; Z = –4.135]. As a result, mean sCort in the passive control group C was significantly higher than initial mean sCort, whereas increases observed in the other two groups were not significant [t3–t1, Wilcoxon Signed Ranks test: p (N) = 0.052; Z = –1.943 vs p (M) = 0.458; Z = –0.743 vs p (C) = 0.001; Z = –3.322].

3.3 Group Comparison of Structural MRI Data

In conjunction with the JuBrain Anatomy Toolbox 3.0 for SPM (Institute of Neuroscience and Medicine, Brain and Mind – INM-7, Forschungszentrum Jülich GmbH, Jülich, North Rhine-Westphalia, Germany; https://www.fz-juelich.de/en/inm/inm-7/resources/jubrain-anatomy-toolbox), our VBM analysis revealed multiple brain regions displaying significant GM density changes in the first two weeks (t2–t1) as well as in the entire four-week interval (t3–t1). Cluster distribution patterns differed significantly between nasal intervention and oral control SPM contrasts (see Tables 1,2,3,4 and Fig. 5).

Table 1. Significant GM differences in the nasal intervention group in contrast to the passive control group (N > C) in the first two-week interval (t2–t1).

Clusters		MNI coordinates			Hemisphere	T value
Size k	Region(s) of cluster	x [mm]	y [mm]	z [mm]		
735	HC (DG, CA1, Subiculum)	–13.5	–33.0	–4.5	left	3.11
376	HC (DG, CA1, Subiculum)	28.5	–30.0	–7.5	right	2.80
51	OFC, BF, pACC (BA 33)	12.0	4.5	–15.0	right	2.62
214	Caudate	12.0	19.5	0	right	2.38
56	HC (CA1, Subiculum)	30.0	–28.5	–21.0	right	2.21
96	Amygdala	–21.0	0	–18.0	left	2.20

Annotations: OFC, orbitofrontal cortex; BF, basal forebrain; pACC, pregenual anterior cingulate cortex; HC, hippocampus (DG, dentate gyrus; CA1, Cornu ammonis region 1); GM, gray matter; MNI, Montreal Neurological Institute; BA 33, brodmann area 33.

Table 2. Significant GM differences in the oral control group in contrast to the passive control group (M > C) in the first two-week interval (t2–t1).

Clusters		Peaks	MNI coordinates			Hemisphere	T value
Size k	Region(s) of cluster	Region(s) of peak	x [mm]	y [mm]	z [mm]		
		Insular lobe					
891	AIns		–27.0	27.0	–3.0	left	3.88
		AIns	–37.5	13.5	–4.5	left	3.19
		AIns	–33.0	6.0	–16.5	left	2.62
422	AIns		42.0	9.0	–10.5	right	3.11
		AIns	37.5	21.0	–10.5	right	2.40
		AIns	30.0	28.5	–1.5	right	2.02
		Limbic lobe					
509	HC (CA1), Amygdala		31.5	–9.0	–22.5	right	2.84
88	HC (DG)		28.5	–33.0	–3.0	right	2.39
54	PHG, HC, EC, HATA		–16.5	–16.5	–27.0	left	2.27
36	PHG		–31.5	–27.0	–22.5	left	2.19
26	HC		–31.5	–12.0	–21.0	left	1.98
124	sACC (BA s24)		1.5	16.5	–10.5	right	2.27
		Basal ganglia					
427	Caudate		12.0	22.5	1.5	right	4.00
376	Caudate		–16.5	21.0	9.0	left	3.07
		Putamen	–22.5	16.5	–3.0	left	2.85
37	Putamen		24.0	13.5	4.5	right	2.38

Annotations: AIns, anterior insular cortex; PHG, parahippocampal gyrus; EC, entorhinal cortex; HATA, hippocampus-amygdala-transition-area; HC, hippocampus (DG, dentate gyrus; CA1, Cornu ammonis region 1); sACC, subgenual anterior cingulate cortex.

Crucially, significant GM density growth across the entire four-week timeline was isolated to the nasal intervention group, remaining absent in both control groups (see Table 5).

3.4 multiple regression Analysis of Structural MRI and Physiological Stress Parameters, and Group-Membership

Using decreasing heart rate as a predictor of structural brain change, the paired multiple regression analysis revealed several clusters in three major zones of increased GM density: (1) brainstem, (2) hippocampus formation, (3) cerebral cortex (see Table 6).

Testing these clusters for group membership, we found that in the first two-week interval the active control group M demonstrated a significant GM density growth in the right amygdala and hippocampus-amygdala-transition-area (HATA) [Wilcoxon Signed Ranks test: p (mouth) = 0.021; Z = –2.306 vs p (nose) = 0.554; Z = –0.606 vs p (passive control) = 0.460; Z = –0.739]. This cluster was also the only one to change significantly in the independent-samples Kruskal-Wallis test (H = 6.243; df = 2; p = 0.044); however, pairwise comparisons did not result in significant group differences (mouth vs nose: Bonferroni adjusted p

Table 3. Significant GM differences in the nasal intervention group in contrast to the oral control group (N > M) in the first two-week interval (t2–t1).

Clusters		MNI coordinates			Hemisphere	T value
Size k	Region(s) of cluster	x [mm]	y [mm]	z [mm]		
131	OFC, BF, pACC (BA 33)	10.5	4.5	–15.0	right	3.92
1957	HC (DG, CA1, Subiculum)	–15.0	–27.0	0	left	3.46
54	HC (Subiculum. CA1)	–24.0	–37.5	–12.0	left	2.44
53	BF (ch4)	–27.0	–13.5	–6.0	left	1.99

Annotations: OFC, orbitofrontal cortex; BF, basal forebrain (ch4, Nucleus basalis Meynert); pACC, pregenual anterior cingulate cortex; HC, hippocampus (DG, dentate gyrus; CA1, Cornu ammonis region 1).

Table 4. Significant GM differences in the oral control group in contrast to the nasal intervention group (M > N) in the first two-week interval (t2–t1).

Clusters		Peaks	MNI coordinates			Hemisphere	T value
Size k	Region(s) of cluster	Region(s) of peak	x [mm]	y [mm]	z [mm]		
		Insular lobe					
228	AIns		31.5	28.5	4.5	right	3.21
1478	AIns		–30.0	15.0	4.5	left	2.95
		Frontal operculum, AIns	–40.5	7.5	7.5	left	2.89
		Frontal operculum, AIns	–31.5	27.0	7.5	left	2.77
494	AIns		40.5	4.5	–9.0	right	2.62
		PIns	43.5	–10.5	6.0	right	2.01
113	Parietal operculum		–40.5	–22.5	19.5	left	2.81
		Limbic lobe					
304	EC		–25.5	–13.5	–33.0	left	2.80
		HC (Subiculum)	–24.0	0	–42.0	left	2.61
628	Amygdala, HATA, HC		27.0	–7.5	–22.5	right	2.77
		Amygdala, HC	19.5	–13.5	–19.5	right	2.58
44	EC		27.0	–3.0	–39.0	right	2.18
38	HATA		–13.5	–18.0	–19.5	left	2.02
47	sACC (BA s24)		3.0	16.5	–10.5	right	2.03
		Basal ganglia					
95	Putamen		–25.5	13.5	1.5	left	2.76
141	Caudate		–14.0	17.0	8.0	left	2.81
107	Caudate		15.0	19.5	10.5	right	2.42

Annotations: AIns, anterior insular cortex; PIns, posterior insular cortex; EC, entorhinal cortex; HATA, hippocampus-amygdala-transition-area; HC, hippocampus; sACC, subgenual anterior cingulate cortex.

= 0.08; z = 2.210; mouth vs passive control: Bonferroni adjusted p = 0.09; z = –2.194). The right HATA and the left dorsal hippocampus formed a significant multinomial regression model for group membership [χ^2 (4) = 13.885; p = 0.008]. Pearson's chi-square test [χ^2 (182) = 185.336; p = 0.417] and Deviance chi-square test [χ^2 (182) = 191.597; p = 0.298] indicated that the model fits the data well. Consequently, the right hippocampus-amygdala transition area emerged as a significant predictor for group membership [mouth vs passive control: b = –42.637; s.e. = 19.111; p = 0.026] [mouth vs nose: b = 43.276; s.e. = 18.600; p = 0.020]. On the other hand, the left dorsal hippocampus qualified as a significant predictor only when discriminating active oral control against membership in the passive control group [mouth vs passive control: b = –143.025; s.e. = 65.255; p = 0.028] [mouth vs nose: b = 109.457; s.e. = 63.865; p = 0.087].

Analysis over the whole four-week interval revealed that only the intervention group N showed a significant GM density increase in the right ventral diencephalon (subthalamic nucleus, STN) [t3–t1, Wilcoxon Signed Ranks test: p (nose) = 0.001; Z = –3.619 vs p (mouth) = 0.101; Z = –1.642 vs p (passive control) = 0.877; Z = –0.154], in addition to a significant GM density increase in the upper right dorsal brainstem (tectum) [t3–t1, Wilcoxon Signed Ranks test: p (nose) = 0.005; Z = –2.785 vs p (mouth) = 0.064; Z = –

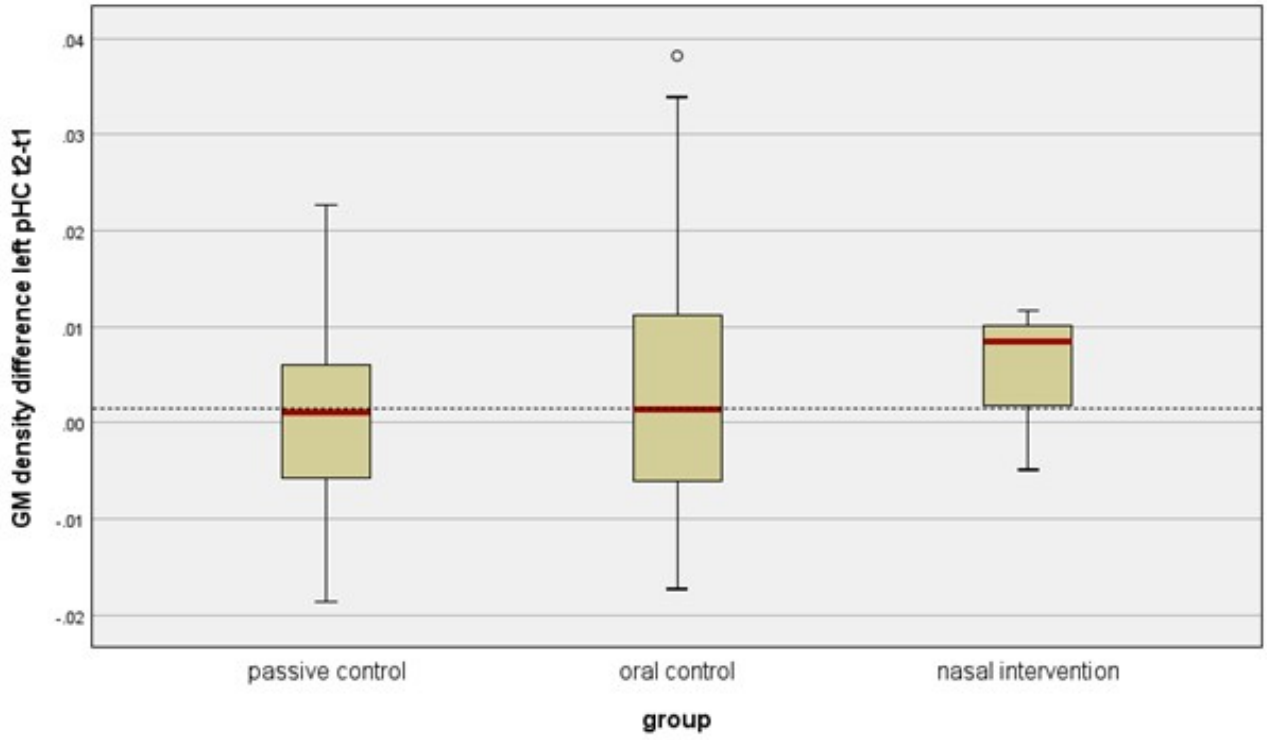


Fig. 5. Difference in GM density in the left posterior hippocampus (pHC) after first two-week interval (t2–t1) across groups. Box = IQR; line = median; whiskers = 1.5 × IQR; ○ = outlier; dotted line = 0.

Table 5. Significant GM differences in the nasal intervention group in contrast to the oral active and passive control groups (N > M, N > C) in the entire four-week interval (t3–t1).

Clusters		Peaks	MNI coordinates			Hemisphere	T value
Size k	Region(s) of cluster	Region(s) of peak	x [mm]	y [mm]	z [mm]		
t3–t1: GM N > M							
64	Ncl. Accumbens		12.0	7.5	–13.5	right	2.64
397	HC (CA1, Subiculum)		–13.5	–28.5	1.5	left	2.15
		Hypothalamus	–12.0	–25.5	–7.5	left	1.94
t3–t1: GM N > C							
139	EC, Amygdala		–21.0	1.5	–24.0	left	2.56
44	OFC		–19.5	6.0	–19.5	left	2.40
38	Caudate		15.0	9.0	9.0	right	2.29
53	AIns		–27.0	15.0	–15.0	left	1.95

Annotations: OFC, orbitofrontal cortex; HC, hippocampus (CA1, Cornu ammonis region 1); EC, entorhinal cortex; AIns, anterior insular cortex.

1.855 vs p (passive control) = 0.185; Z = –1.327]. However, in the subsequent independent-samples Kruskal-Wallis test (H = 8.581; df = 2; p = 0.014), only the GM density increase in the right STN cluster differed significantly across groups, more precisely between group N and C (Bonferroni adjusted p = 0.013; z = –2.851). Similarly, the right STN was also the only cluster to predict group membership significantly over the four-week period [χ^2 (2) = 6.493; p = 0.039].

In a paired whole-brain multiple regression analysis decreasing salivary cortisol levels (sCort) predicted a set of five significant cortical clusters of increased GM density, in the first two-week interval (see Table 7).

On closer inspection, only the GM density increases observed in the intervention group N proved to be significant in the following three cluster regions:

- Inferior parietal lobule/ supramarginal gyrus (MNI coordinates [x y z] = –55.5, –45, 40.5) [Wilcoxon Signed Ranks test: p (nose) = 0.027; Z = –2.211 vs p (mouth) = 0.885; Z = –0.144 vs p (passive control) = 0.340; Z = –0.954].

Table 6. Regions of the brain with significant GM density growth predicted by decreasing heart rate in two (t2–t1) and four weeks (t3–t1).

Clusters		Peaks	MNI coordinates			Hemisphere	T value
Size k	Region(s) of cluster	Region(s) of peak	x [mm]	y [mm]	z [mm]		
t2–t1: GM ↑ HR ↓							
Brainstem							
1154	Brainstem		0	–39.0	–30.0	paramedian-right	6.36
		Pons	9.0	–34.5	–51.0	paramedian-right	5.86
		Medulla oblongata	1.5	–43.5	–45.0	paramedian-right	5.47
42	Ventral brainstem	Mesencephalon	1.5	–13.5	–27.0	paramedian	4.41
Hippocampus							
90	HC (pHC)		27.0	–46.5	18.0	right	5.25
		pHC	16.5	–39.0	21.0	right	5.17
		pHC	25.5	–37.5	21.0	right	3.97
38	HC (pHC)		–16.5	–43.5	19.5	left	4.06
		pHC	–13.5	–34.5	22.5	left	3.26
254	HATA (HC, Amygdala)		33.0	–4.5	–30.0	right	4.79
		HC (CA1)	34.5	–10.5	–19.5	right	3.86
Cerebral cortex							
130	ITG		57.0	–42.0	–18.0	right	4.51
128	POS, precuneus		22.5	–73.5	37.5	right	4.27
		SOG, cuneus	19.5	–78.0	31.5	right	4.23
t3–t1: GM ↑ HR ↓							
27	Dorsal brainstem	Mesencephalon	13.5	–30.0	–7.5	right	3.84
138	Ventral diencephalon		3.0	–9.0	–6.0	paramedian-right	3.63
		STN, VL	6.0	–19.5	–1.5	right	3.50

Annotations: ↑, increase; ↓, decrease; HC, hippocampus (pHC, posterior hippocampus); HATA, hippocampus-amygdala-transition-area; ITG, inferior temporal gyrus; POS, parieto-occipital sulcus; SOG, superior occipital gyrus; STN, subthalamic nucleus; VL, ventrolateral thalamus. Note that the final brainstem clusters were extracted in approximation to the coordinates of the three main respiratory groups of the brainstem: VRG, ventral respiratory group (MNI coordinates [x y z] = 2, –35, –48), DRG, dorsal respiratory group (MNI coordinates [x y z] = 2, –44, –45), PRG, pontine respiratory group (MNI coordinates [x y z] = 0, –39, –30).

Table 7. Regions of the brain with significant GM density increase predicted by decreasing salivary cortisol levels in two weeks (t2–t1).

Clusters		Peaks	MNI coordinates			Hemisphere	T value
Size k	Region(s) of cluster	Region(s) of peak	x [mm]	y [mm]	z [mm]		
t2–t1: GM ↑ sCort ↓							
912	IPL, SMG		–55.5	–45.0	40.5	left	4.30
		Angular gyrus	–43.5	–58.5	48.0	left	4.01
		Postcentral gyrus	–58.5	–22.5	46.5	left	3.51
379	SFG		–25.5	–4.5	55.5	left	4.07
		Precentral gyrus	–43.5	0	52.5	left	3.72
		Precentral gyrus	–48.0	1.5	45.0	left	3.53
129	MFG		–49.5	18.0	31.5	left	3.77
		MFG	–48.0	25.5	34.5	left	3.48
108	Precuneus		6.0	–73.5	52.5	right	3.77
36	SPL		–1.5	–40.5	73.5	left	3.41
		Postcentral gyrus, precuneus	–7.5	–51.0	73.5	left	3.29

Annotations: ↑ (increase), ↓ (decrease), IPL, inferior parietal lobule; SMG, supramarginal gyrus; SFG, superior frontal gyrus; MFG, middle frontal gyrus; SPL, superior parietal lobule.

- Middle frontal gyrus (MFG coordinates [x y z] = –49.5, 18, 31.5) [Wilcoxon Signed Ranks test: p (nose) = 0.018; Z = –2.366 vs p (mouth) = 0.178; Z = 1.346 vs p (passive control) = 0.575; Z = –0.561].
- Superior parietal lobule (MNI coordinates [x y z] = –1.5, –40.5, 73.5) [Wilcoxon Signed Ranks test: p (nose) = 0.036; Z = –2.097 vs p (mouth) = 0.249; Z = 1.153 vs p (passive control) = 0.085; Z = –1.720].

However, only the GM density increase of the middle frontal gyrus differed significantly in the inter-group comparison (independent-samples Kruskal-Wallis test: H = 7.050; df = 2; p = 0.029), with pairwise comparison confirming that specifically the intervention group N differed from the other two groups in a significant manner (nose vs passive control: Bonferroni adjusted p = 0.042; z = 2.458, nose vs mouth: Bonferroni adjusted p = 0.043; z = 2.448). Additionally, the GM density dynamics in the middle frontal gyrus (MNI see above) and the superior parietal lobule (MNI see above) proved to be two significant predictors for group membership in a robust multinomial regression model [χ^2 (4) = 15.474; p = 0.004], which fitted the data well [Pearson's χ^2 (182) = 181.960; p = 0.482 and Deviance χ^2 (182) = 190.008; p = 0.327].

Multiple regression analyses with independent blood pressure variables failed to produce any significant and/or meaningful clusters.

3.5 Harms and Adverse Events

Systematic inquiry across all three measurement appointments yielded no serious adverse events in any group. No MRI-related adverse events or incidental findings necessitating clinical follow-up occurred.

4. Discussion

This longitudinal intervention study contrasted four weeks of daily nasal *pranayama* with an active oral and a non-exercising passive control group. Contrary to the control groups, two weeks of nasal respiratory training produced significant group-specific structural MRI changes in stress-sensitive brain areas, e.g., medial prefrontal cortex and hippocampal formation, with corresponding changes in neurohumoral and neurovegetative surrogate parameters of the stress response, such as salivary cortisol levels and heart rate.

4.1 Neurohumoral and Neurovegetative Effects of pranayama: A Short Neurophysiology of Conscious Breathing and Stress

The neurophysiological crosstalk between conscious breathing, the peripheral, and central nervous systems comprises multiple layers of complex regulatory interactions; consequently, we recognize that the present sMRI-based work can only discuss our neurohumoral and neurovegetative findings in a limited overview of this topic.

Fundamentally, central respiratory control can be subdivided into two regulatory circuits [35]:

1. a volitional top-down pathway originating from frontocortical and subcortical cognitive circuits, localized predominantly within the limbic system, and
2. an automatic system driving spontaneous rhythm generation via the respiratory central pattern generator (rCPG) alongside autonomic integration in the brainstem.

Most of the time, we do not pay attention to our breathing patterns and do not exert volitional control. However, both volitional and autonomic circuits co-regulate each other through bidirectional interaction with the CNS and the periphery. Modulatory CNS influences may include higher-order integrative processes, such as emotional stress, but also neurohumoral pathways, such as inflammatory mediators or steroid-based signalling (cortisol) [36].

Peripheral input reaches the brain through a wide array of vagal and glossopharyngeal feedback pathways involving information from mechanosensory receptors in the airways, thorax, and respiratory muscles as well as chemosensory receptors (O_2, CO_2, pH) in the brainstem, carotid, and aortic bodies [36]. Considerable scientific attention in the field of conscious breathing exercises has been directed toward the effects of transient hypoxia on respiratory neuroplasticity [37,38,39] and autonomic brain reflex sensibility [40,41,42]. Aware of this potential confounder, we tested our respiratory paradigm for variations in blood oxygen saturation via pulse oximetry in the context of our pilot fMRI study and failed to detect any significant changes [M. Garner & C. Krick, personal communication, 2020]. Consequently, we did not pursue this modality in the design of the present study. To optimize experimental rigor, future protocols could, however, isolate these chemosensory confounders through the implementation of capnography, pulse oximetry, or more invasive instruments.

A compelling observation in the face of this complexity is that literature still lacks a definitive consensus on the directionality of the mechanisms underlying the effects of distinct conscious breathing exercises on physiological stress parameters. For instance, it remains unclear whether nasal *pranayama* initially modulates higher-order autonomic stress circuits in the CNS to regulate peripheral neurohumoral and neurovegetative effector pathways via top-down signaling, or whether its autonomic effects originate from the direct modulation of peripheral neurophysiological feedback loops that subsequently influence central stress circuits through bottom-up projections [35,43]. Acknowledging the importance of both mechanisms, we argue that neither model independently explains the multi-system differences observed between the nasal intervention group and controls in our study. Accordingly, we address the peripheral bottom-up perspective in a separate work [Hübner, R., personal communication, 2025], dedicating the current paper to isolating top-down regulatory pathways of the

stress-relaxation response, including the potential role of direct non-odorant mechanosensory input from the nasal epithelium [44].

As a major methodological constraint, our longitudinal intervention design leaves the respective effects of slow and fast nasal breathing experimentally confounded, specifically with regard to their individual effects on physiological stress parameters. Future protocols could resolve these confounding factors by systematically isolating each breathing rate, building upon the exploratory insights of this and previous works.

For example, deep, slow nasal breathing with low inhalation/exhalation ratios, comparable to *dirgha pranayama*, has been found to improve cardiovascular health and neurovegetative stress resilience, by increasing long-term heart rate variability and reducing mean heart rate [43,45,46,47,48,49], ultimately promoting cardiovagal dominance over sympathetic efferents in prolonged practice over several weeks [50]. Conversely, respiratory exercises involving controlled hyperventilation, like *vatakrama kapalbhati*, elicit a biphasic response: an initial, acute induction of sympathetic arousal and parasympathetic withdrawal, followed by a compensatory post-exercise parasympathetic counter-regulation that significantly enhances overall heart rate variability [51,52,53].

Our findings could indicate a similar synergistic mechanism, wherein the initial controlled hyperventilation segment primes a subsequent parasympathetic relaxation response. Accordingly, the significant group-specific decrease in mean heart rate observed in the nasal intervention group after the first two-week interval could indicate a shift in autonomic nervous homeostasis in favor of stress reduction. Concurrently, the synchronized decline in mean salivary cortisol levels during this same period points toward a significant downregulation of the hypothalamic-pituitary-adrenal (HPA) stress axis.

The mechanisms behind the rebound in mean heart rate and salivary cortisol levels during the final two-week interval remain partially unresolved. While habituation to an invariant *pranayama* protocol offers a plausible explanation, it fails to fully account for the parallel elevation observed in the passive control cohort, which ultimately exceeded its baseline metrics. Beyond habituation, psychological shifts may have influenced these trends: initial engagement driven by study novelty may have transitioned over time into participant fatigue, with the final assessment period being perceived as mildly tedious or distressing. Subsequent studies would benefit from systematically assessing the role of intrinsic motivation, as well as investigating whether a more varied respiratory protocol could amplify effect sizes by maintaining engagement and optimizing long-term compliance.

Data concerning blood pressure parameters presented a higher degree of ambiguity and interpretive complexity. While available literature indicates that nasal *pranayama* predictably reduces mean diastolic blood pressure [43], the concurrent reduction observed in our oral control group lacks empirical precedent and plausibility in the wider associative framework of subsequent regression analyses. Conceptually, an elevation in blood pressure represents a more predictable physiological response to oral breathing, given the potential homeostatic disruption and discomfort associated with this innately unphysiological breathing. Reflecting this, current literature primarily evaluates the role of oral breathing in pathological states, notably arterial hypertension [54,55] as well as respiratory and neuropsychiatric conditions in children [56]. This divergence in our findings could indicate the presence of mechanistic or methodological confounders in the oral control group, potentially linked to considerations regarding intragroup variance and heterogeneity discussed below.

4.2 Group Comparison of Structural CNS Changes: Functional MRI Predicting GM Density Changes in the Hippocampus

Before proceeding to the discussion of our MRI findings, some methodological considerations are in order. Despite all necessary and well-established pre-processing steps, VBM alone cannot be used to confidently infer microscopic cellular processes from statistical macroscopic findings [30]. The underlying causes for the observed GM density changes are most likely multifactorial, representing local synaptic events, such as synaptogenesis or synaptic pruning, gliagenesis, neurogenesis but also angiogenesis, cell size fluctuations, and changes in interstitial or glymphatic flow [57]. Therefore, neuroplasticity is one of many potential explanations for the observed structural VBM effects and must be considered in conjunction with other measurement modalities, such as fMRI.

At its core, VBM analysis involves the use of multiple comparisons via the General Linear Model which is associated with an elevated risk of false positives. While we successfully performed the conservative Family-Wise Error (FWE) correction for our fMRI findings, the VBM study was ultimately not sufficiently powered to benefit from the high specificity and low sensitivity of FWE. Guided by a growing body of literature and our fMRI pilot findings [M. Garner & C. Krick, personal communication, 2020], we instead limited the amount of compared voxels in the group comparison analysis through ROIs and prioritized sensitivity to small changes in gray matter density architecture in accordance with a less conservative exploratory approach.

The resulting significant GM density increases in the bilateral hippocampus formation, basal forebrain, parts of the orbitofrontal and medial prefrontal cortices, exclusive to the nasal intervention group N, evoke a pattern of neuromorphological transformation along the primary and secondary endings of the olfactory tracts.

In particular, the multimodal hippocampus formation constitutes a major site of adult structural neuroplasticity

with a high degree of internal and external connectivity enabling a wide range of integrative functions, such as memory consolidation, spatiotemporal coordination, regulation of emotion, and, crucially, central stress-relaxation circuits [58]. Accordingly, mindfulness, meditation, and MBI studies have consistently shown functional and structural MRI changes involving the hippocampus [20,31,59,60,61].

Here, functional MRI data acquired by [Reckner, T., personal communication, 2025] during our first and second measurement appointments played an important role in supplementing the interpretation of the VBM group analysis in several ways.

Whilst the final VBM analysis could not differentiate between slow and fast nasal breathing with regards to the observed structural effects, activation changes seen in fMRI could clearly be attributed to distinct respiratory frequencies and airway routes used (nose vs mouth). This was particularly relevant for findings pertaining to the Default Mode Network (DMN). For instance, Reckner et al. [Reckner, T., personal communication, 2025] found that slow nasal breathing, not fast nasal breathing, nor any frequency of oral breathing, resulted in significant activation changes of the left (posterior) hippocampus and precuneus/posterior cingulate cortex (PCu/PCC) regions during the first measurement appointment. Activation pattern changes in these regions independently predicted the GM density increase in the left hippocampus of the nasal intervention group N after two weeks. Hence, the continuity and association between structural and functional findings can be seen as a multimodal indication of sustained and consistently localized plasticity occurring in the hippocampal region.

The concentration of the most significant GM density clusters and fMRI activation in the left posterior hippocampus should also be considered in the topographical context of a functional anterior-posterior gradient [62,63]. For instance, histochemical studies show that the posterior hippocampus communicates with the basal forebrain complex via a distinct cholinergic circuit involved in associative olfactory tract mediated learning [64]. At the same time, relaxation-based mindfulness and MBI studies provide structural as well as functional MRI evidence of consistent connectivity and coactivation of the posterior hippocampus with key DMN structures, like the precuneus [10,13].

Regular nasal respiratory exercise could similarly contribute to a form of learned relaxation through DMN modulation. While our study is likely the first to illuminate this prospect from an MRI perspective of high spatial resolution, high temporal resolution EEG studies have already demonstrated that slow nasal breathing, unlike slow oral breathing, can modulate DMN activity through distinct bands of olfactory tract mediated oscillations and induce changes in subjectively perceived states of consciousness [65].

In contrast, the most significant GM density differences of the oral control group clustered in the right amygdala, which is more involved in processing negative emotions [66] as well as aversive stimuli, like pain and dyspnea, in conjunction with the insula [67]. Subjective discomfort and stress in the face of regular and innately unphysiological mouth breathing could thus have contributed to structural changes in aversive learning hubs, like the amygdala [68,69]. Similarly, the GM density increase in the subgenual anterior cingulate cortex (sACC, BA s24), a region related to negative feelings, is directly contrasted by the GM density increase in the pregenual anterior cingulate cortex (pACC, BA 33) of the nasal intervention group, a region active in positive emotional awareness, pleasure and reward processing [70,71].

The involvement of the right anterior hippocampus and HATA can be interpreted in terms of their proximity to the right amygdala and hippocampal functional topography, where they play an important role in the stress response and context-dependent processing of emotion [63,72]. These findings must, however, be weighed against the backdrop of high intragroup variance for this region in the oral control group M, overlapping with some significant right-sided hippocampal GM density clusters (N > C). This overlap did not occur during the functional MRI experiment, neither on the first nor the second appointment, where only the slow nasal breathing condition consistently activated the hippocampus. Right-sided hippocampal clusters are also notably absent in GM density contrasts examining the entire four-week interval. Here, the oral control group did not show any significant GM density group differences, whereas the left hippocampal formation of the nasal intervention group still showed significant differences in GM density growth (N > C, N > M). Therefore, the exact group significance of the right hippocampus and amygdala for oral respiratory exercises are yet to be established. Future higher-powered longitudinal structural MRI studies could investigate whether elevated intragroup variance is inherent to mouth breathing or whether it can be reduced by more rigorous airway control during oral breathing exercises (e.g., nose clamps) at the risk of increasing aversive stressful confounders.

4.3 Structural CNS Findings Through the Lens of Neurohumoral and Neurovegetative Predictors

Considering the notable intragroup variance of the oral control group discussed above, we performed an additional exploratory paired multiple regression analysis with physiological stress covariates in order to supplement the observed structural group differences and better isolate regression-based associations between neuromorphology and the peripheral stress response.

Significant HR-associated structural changes in brainstem GM density are consistent with the concept of *pranayama*-induced cardiorespiratory integration between major respiratory centers, like the dorsal, ventral medullary

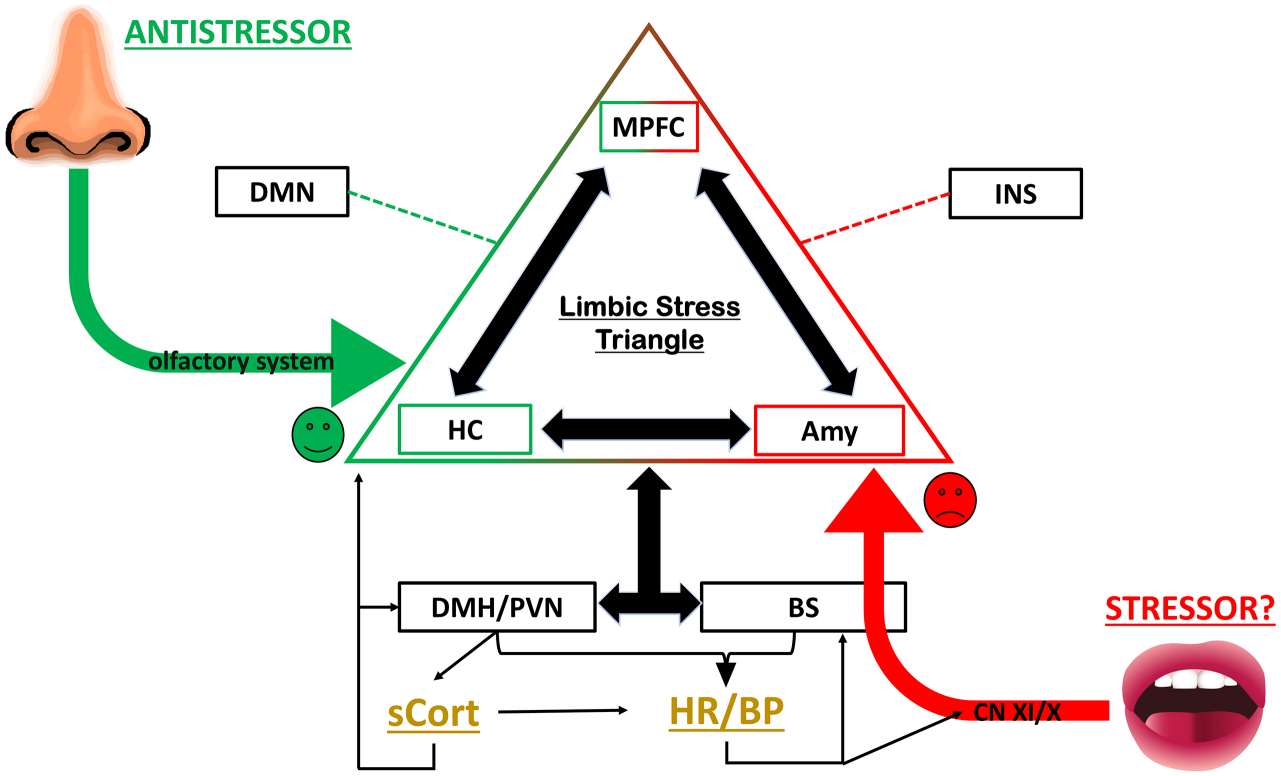


Fig. 6. Overview of limbic stress regulation and neuromorphological change in response to nasal (antistressor, green) and oral breathing (potential stressor, red). Nasal respiratory exercises (*pranayama*) may influence the regulatory limbic stress triangle via mechanical olfactory input. The structural equilibrium of the limbic stress triangle can shift toward neuromorphological changes within the left posterior hippocampus (HC), medial prefrontal cortex (mPFC), and associated default mode network (DMN) structures, thereby attenuating the pro-stress regulatory influence of the right amygdala (Amy), the hippocampus-amygdala transition area, and the anterior hippocampus. Oral respiratory exercises might have stimulated structural changes in the pro-stress limb of the triangle through indirect, bottom-up vagal (CN X) input to the brainstem (BS), which relays it to the amygdala and associated anterior insular cortex (INS). The limbic stress triangle maintains bidirectional connections with the dorsomedial hypothalamus/paraventricular nucleus (DMH/PVN) and BS. The latter two give rise to changes in salivary cortisol levels (sCort), heart rate (HR) and blood pressure (BP) in accordance with a pro- or anti-stress disposition of the limbic stress triangle. Cortisol levels covary with and exert central negative feedback on the limbic stress triangle and DMH/PVN. Glucocorticoids also increase HR/BP peripherally. A rise in HR and BP results in negative feedback inhibition of the respective cardiovascular brainstem centers through neurovegetative reflex loops.

and pontine groups, as well as cardiovascular pressor-depressor centers [73]. One explanation for the lack of group-specificity in this region could be that both oral and nasal respiratory exercises stimulate cardiorespiratory neuroplasticity in key brainstem centers, like the pre-Bötzinger complex and nucleus tractus solitarii [73]. The right amygdala, anterior hippocampus and the transitional zone in between (HATA) could represent an instance of stress-related feed-forward regulation of the cardiovascular system in the context of the wider central autonomic network (CAN) [74]. As discussed in the previous section, this region warrants further investigation to disentangle its potential role in relaying the effects of conscious breathing exercises on autonomic stress response parameters.

Finally, only the nasal intervention group registered a group-specific GM density increase in the ventral hypothalamus after four weeks. This could point toward a structural reorganization of autonomic effector pathways in the dorsomedial and paraventricular hypothalamus but more research is needed to explore this association.

As for sCort-associated multiple regression outcomes, the increase in GM density was most significant and specific for nasal *pranayama* in the medial prefrontal cortex (mPFC); a region whose structural and functional neuroplasticity are strongly susceptible to changing glucocorticoid levels [75]. The mPFC performs higher-order coordination of stress-relaxation responses by aligning HPA, autonomic nervous system (ANS), and behavioral adaptations in concert with the hippocampus, amygdala, and brainstem [76].

Consistently with these higher-order stress response circuits, the GM density increase in the left posterior hip-

pocampus, specific to the nasal intervention group, was associated with reduced mean and baseline sCort during the first two-week interval. Comparable sCort associations could be isolated for this region based on our functional MRI data. Similarly to the mPFC, hippocampal plasticity and sCort have long been known to be coupled in a mutual, bidirectional feedback loop [77]. For instance, the hippocampus exerts a distinct tonic feedback inhibition on the paraventricular nucleus of the hypothalamus [78]. Conversely, a high density of glucocorticoid and mineralocorticoid receptors predisposes the HC to lose structural plasticity with elevated glucocorticoid levels but also to recover with stress relief [79].

Additionally, increased GM density in DMN structures of the nasal intervention group, like the superior parietal lobule and precuneus, were associated with decreased mean sCort over the first two-week period (see Table 7).

Collectively, these relationships could further substantiate the role of nasal *pranayama* in driving autonomic relaxation and concurrent structural VBM changes. However, we recognize that the associative nature of these findings can only serve as an exploratory starting point for future multimodal studies. Likewise, characterizing possible residual neurohumoral and neurophysiological confounders at the central-peripheral nervous system interface could be an important avenue for future investigation, e.g., the brain pathways of the renin–angiotensin–aldosterone system [80] or central sensorimotor and autonomic brainstem reflex loops [81,82,83].

4.4 The Limbic Stress Triangle

Taken together, our multimodal empirical evidence, encompassing structural and functional MRI alongside neurohumoral and neurovegetative outcomes of conscious nasal versus oral breathing, emphasizes bidirectional top-down and bottom-up regulatory circuits centered on the hippocampus, amygdala, and medial prefrontal cortex (mPFC). As described by Mah et al. [84] in the context of anxiety disorders, this triangular limbic subsystem constitutes the regulatory backbone of the stress response. In their proposed model, an anti-stress, top-down, dorsoventral pathway involving the hippocampus and mPFC counterbalances a pro-stress, amygdala-based, bottom-up, ventral pathway.

Based on our own findings, we propose that nasal *pranayama* could function as a nonpharmacological antistressor stimulus for structural transformation in the HC-mPFC tandem [85] via non-odorant mechanical signaling along the olfactory pathway [65,86,87]. Here, the left posterior hippocampus could serve as a critical functional hub within the default mode network (DMN), demonstrating important co-activation with parietal associative regions. Functional and structural MRI changes in the HC-mPFC tandem were likewise associated with reduced physiological stress parameters and could represent a rebalancing of central neural networks, like the DMN, toward a more relaxed, mindful disposition [14,88]. However, we acknowledge that further multimodal empirical validation is needed to definitively answer the question of directionality and causality in the complex relationship between conscious nasal breathing and the limbic stress triangle. Therefore, the overview shown below (see Fig. 6) is not intended to imply causality but to demonstrate a simplified explanatory framework of relevant CNS structures, their bidirectional interactions, and crosstalk with physiological effector parameters of the stress response.

In contrast, evidence regarding conscious oral breathing was less conclusive and complicated by intragroup variability, precluding a definitive characterization with regards to the limbic stress triangle. Unlike the nasal intervention group, structural changes in the oral control group were characterized by a scattered distribution of increased GM density around the right amygdala and insular cortex, either driven by indirect, bottom-up vagal inputs to thalamo-cortico-subcortical circuits [89] or resulting from intrinsic discomfort in the face of unphysiological mouth breathing. Although the link to stressful arousal appears theoretically sound, none of these structural changes showed convincing evidence of group-specific correlation with physiological stress parameters or functional MRI findings.

5. Conclusions

Daily nasal *pranayama*, involving deep controlled hypoventilation, alters the structural composition of key stress-sensitive brain regions, such as the hippocampus, a process potentially mediated through a distinct olfactory pathway. These structural effects are associated with functional activation changes in default mode network structures as well as decreases in neurovegetative and neurohumoral stress parameters during the first two-week interval. By contrast, the oral intervention group exhibited distinct structural gray matter changes that did not significantly correlate with changes in physiological stress parameters or fMRI. Finally, our data suggest a temporal limit to the effects of invariant *pranayama* training. Beyond a two-week threshold, a reduced signal-to-noise ratio combined with progressive habituation to the training stimulus appears to lower the impact of our nasal respiratory paradigm, a factor that must be accounted for in future respiratory intervention protocols.

Clinical Implications

Yoga-related complementary therapies have been successfully employed in various medical contexts, e.g., chronic pain syndromes, neuropsychiatric, cardiovascular, and autoimmune disorders [90,91,92,93,94]. However, elderly, less mobile and critically ill patients may not be able to perform physical postures (asanas). Our research shows that simple respiratory exercises (*pranayama*) could have similar neuro- and cardioprotective effects through a de-

crease in stress and an increase in structural neuroplasticity. Future studies should further examine this hypothesis in the clinical setting.

6. Limitations

- Randomization process: Participants were assigned to their respective group via random number generator. A prior inquiry about personal preferences and potential vetoes was considered for better compliance, although only a select few cases were impacted by this. Since only relative differences were prioritized, intrapersonal constants had no bearing on the paired testing design.
- Lack of complete double-blinding due to methodological considerations.
- External validity: This study's sample was mostly composed of young healthy students from a high-stress university environment. It remains to be examined whether similar vegetative and neuroplastic effects can be shown in the elderly and sick for instance.
- VBM cannot be used to definitively resolve microscopic tissue alterations on the cellular level. Neuroplastic processes are one of various explanations for the observed GM density changes. However, observations in animal models have depicted synaptogenesis [95] and neurogenesis [96] as key mechanisms in adult neuroplasticity. Given the relatively short duration of the intervention interval, caution is therefore warranted not to overstate the weight of long-term processes, like neurogenesis.
- While fMRI data were sufficiently powered for Family-Wise Error correction, the exploratory VBM analysis lacked power to benefit from FWE. We partially mitigated the risk of false positives by limiting the amount of voxels compared. However, the level of significance must be improved in future studies through a greater number of participants.
- The oral control group revealed considerable challenges regarding intragroup variance and interpretability of the results. Future interventional designs should reexamine the suitability of conscious mouth breathing as a control group and aim to elucidate the discrepancy between intra- and intergroup effects. In particular, the use of nose clips should be considered in future longitudinal designs, while explicitly addressing subject discomfort as a potential confounding variable.
- In order to evaluate the participants' long-term stress level prior and posterior to the intervention, we attempted to utilize the Recovery-Stress Questionnaire (RESTQ). However, a different, more flexible questionnaire, such as State-Trait Anxiety Inventory (STAI), could have been a more suitable and flexible choice for measuring general and systemic baseline stress.

Availability of Data and Materials

The datasets used and analyzed during the current study are available from the corresponding authors on reasonable request.

Author Contributions

AS, TR, RH designed the research study and performed the research. AS analyzed the structural VBM data and related it to physical stress parameters. TR, RH focused on evaluation of functional MRI data and salivary cortisol findings in separate doctoral theses. CK provided indispensable assistance and guidance with research, organization, writing, data interpretation, and management of funds. CK and WR acted as supervisors, with a substantial contribution to the conceptualization, design, and subsequent analysis of data. AS wrote the present manuscript with editorial contributions from all authors. All authors read and approved the final manuscript. All authors have participated sufficiently in the work and agreed to be accountable for all aspects of the work.

Ethics Approval and Consent to Participate

Approved by the Ethics Committee of the Saarland Medical Association, approval no. 48/21. This study was approved by the Ethics Committee of the Saarland Medical Association and retrospectively registered via the German Clinical Trials Register with all due transparency regarding data, methodology, and underlying administrative delays in the registration. In accordance with international guidelines and ethical requirements, neither the data nor the methodology nor the initial hypotheses have been altered in the process. The study was carried out in accordance with the guidelines of the Declaration of Helsinki. All participants provided written informed consent prior to enrolment.

Acknowledgment

Dr. med. Malvina Garner for intellectual and technical assistance.

Funding

Saarland University (Committee of Research), Karl and Veronica Carsten foundation (C 2042303 0 1).

Conflicts of Interest

The authors declare no conflicts of interest.

Supplementary Material

Supplementary material associated with this article can be found, in the online version, at https://doi.org/10.31083/JIN50889.

References

[1] Chandla SS, Sood S, Dogra R, Das S, Shukla SK, Gupta S. Effect of short-term practice of pranayamic breathing exercises on

cognition, anxiety, general well being and heart rate variability. Journal of the Indian Medical Association. 2013; 111: 662–665.
[2] Giridharan S, Pandiyan B, Kumar NV, Soumian S. Effects of Pranayama on Cancer Patients: A Narrative Review of Clinical Outcomes. Cureus. 2024; 16: e54688. https://doi.org/10.7759/cureus.54688
[3] Joshi AM, Raveendran AV, Arumugam M. Therapeutic role of yoga in hypertension. World Journal of Methodology. 2024; 14: 90127. https://doi.org/10.5662/wjm.v14.i1.90127
[4] Sharma H, Swetanshu, Singh P. Role of Yoga in Cardiovascular Diseases. Current Problems in Cardiology. 2024; 49: 102032. https://doi.org/10.1016/j.cpcardiol.2023.102032
[5] Varne SR, Balaji PA. A systematic review on molecular, bio-chemical, and pathophysiological mechanisms of yoga, pranayama and meditation causing beneficial effects in various health disorders. Indian Journal of Integrative Medicine. 2023; 3: 87–96.
[6] Das RR, Sankar J, Kabra SK. Role of Breathing Exercises in Asthma-Yoga and Pranayama. Indian Journal of Pediatrics. 2022; 89: 174–180. https://doi.org/10.1007/s12098-021-03998-w
[7] Bentley TGK, D'Andrea-Penna G, Rakic M, Arce N, LaFaille M, Berman R, et al. Breathing Practices for Stress and Anxiety Reduction: Conceptual Framework of Implementation Guidelines Based on a Systematic Review of the Published Literature. Brain Sciences. 2023; 13: 1612. https://doi.org/10.3390/brainsci13121612
[8] R P, Kumar AP, Dhamodhini KS, Venugopal V, Silambanan S, K M, et al. Role of yoga in stress management and implications in major depression disorder. Journal of Ayurveda and Integrative Medicine. 2023; 14: 100767. https://doi.org/10.1016/j.jaim.2023.100767
[9] Campelo G, de Araújo JR, Aristizabal JP, de Souza W, de Castilho GM. Long-term effects of yoga-based practices on neural, cognitive, psychological, and physiological outcomes in adults: a scoping review and evidence map. BMC Complementary Medicine and Therapies. 2025; 25: 92. https://doi.org/10.1186/s12906-025-04825-x
[10] van Aalst J, Ceccarini J, Demyttenaere K, Sunaert S, Van Laere K. What Has Neuroimaging Taught Us on the Neurobiology of Yoga? A Review. Frontiers in Integrative Neuroscience. 2020; 14: 34. https://doi.org/10.3389/fnint.2020.00034
[11] Veerakannan S. Yoga Effects on Brain Health: A Systematic Review of the Current Literature. Aathiyoga Indian Journal of Ancient Medicine and Yoga. 2025; 1: 171–192. https://doi.org/10.63300/4wc67k20
[12] Gomutbutra P, Yingchankul N, Chattipakorn N, Chattipakorn S, Srisurapanont M. The Effect of Mindfulness-Based Intervention on Brain-Derived Neurotrophic Factor (BDNF): A Systematic Review and Meta-Analysis of Controlled Trials. Frontiers in Psychology. 2020; 11: 2209. https://doi.org/10.3389/fpsyg.2020.02209
[13] Leow Y, Rashid NLBA, Klainin-Yobas P, Zhang Z, Wu XV. Effectiveness of mindfulness-based interventions on mental, cognitive outcomes and neuroplastic changes in older adults with mild cognitive impairment: A systematic review and meta-analysis. Journal of Advanced Nursing. 2023; 79: 4489–4505. https://doi.org/10.1111/jan.15720
[14] Calderone A, Latella D, Impellizzeri F, de Pasquale P, Famà F, Quartarone A, et al. Neurobiological Changes Induced by Mindfulness and Meditation: A Systematic Review. Biomedicines. 2024; 12: 2613. https://doi.org/10.3390/biomedicines12112613
[15] Raichle ME, MacLeod AM, Snyder AZ, Powers WJ, Gusnard DA, Shulman GL. A default mode of brain function. Proceedings of the National Academy of Sciences of the United States of America. 2001; 98: 676–682. https://doi.org/10.1073/pnas.98.2.676
[16] Santaella DF, Balardin JB, Afonso RF, Giorjiani GM, Sato JR, Lacerda SS, et al. Greater Anteroposterior Default Mode Network Functional Connectivity in Long-Term Elderly Yoga Practitioners. Frontiers in Aging Neuroscience. 2019; 11: 158. https://doi.org/10.3389/fnagi.2019.00158
[17] Vishnubhotla RV, Radhakrishnan R, Kveraga K, Deardorff R, Ram C, Pawale D, et al. Advanced Meditation Alters Resting-State Brain Network Connectivity Correlating With Improved Mindfulness. Frontiers in Psychology. 2021; 12: 745344. https://doi.org/10.3389/fpsyg.2021.745344
[18] Anand A. Neuroscience of Yoga: Theory and Practice: Part 1. Springer Nature Singapore: Singapore. 2024. https://doi.org/10.1007/978-981-97-2851-0
[19] Jung JY, Park CA, Lee YB, Kang CK. Investigation of Functional Connectivity Differences between Voluntary Respirations via Mouth and Nose Using Resting State fMRI. Brain Sciences. 2020; 10: 704. https://doi.org/10.3390/brainsci10100704
[20] Garner M, Reith W, Krick C. 10-week Hatha Yoga increases right hippocampal density compared to active and passive control groups: a controlled structural cMRI study. Journal of Neuroimaging in Psychiatry and Neurology. 2019; 4: 1–11. https://doi.org/10.17756/jnpn.2019-027
[21] Dodich A, Zollo M, Crespi C, Cappa SF, Laureiro Martinez D, Falini A, et al. Short-term Sahaja Yoga meditation training modulates brain structure and spontaneous activity in the executive control network. Brain and Behavior. 2019; 9: e01159. https://doi.org/10.1002/brb3.1159
[22] Gaser C, Dahnke R, Thompson PM, Kurth F, Luders E, The Alzheimer's Disease Neuroimaging Initiative. CAT: a computational anatomy toolbox for the analysis of structural MRI data. GigaScience. 2024; 13: giae049. https://doi.org/10.1093/gigascience/giae049
[23] Ashburner J, Friston KJ. Why voxel-based morphometry should be used. NeuroImage. 2001; 14: 1238–1243. https://doi.org/10.1006/nimg.2001.0961
[24] Ashburner J, Friston KJ. Voxel-based morphometry–the methods. NeuroImage. 2000; 11: 805–821. https://doi.org/10.1006/nimg.2000.0582
[25] Kurth F, Luders E, Gaser C. Voxel-Based Morphometry. In Toga AW (ed.) Brain Mapping (pp. 345–349). Academic Press: Waltham. 2015. https://doi.org/10.1016/B978-0-12-397025-1.00304-3
[26] Ashburner J, Friston KJ. Unified segmentation. NeuroImage. 2005; 26: 839–851. https://doi.org/10.1016/j.neuroimage.2005.02.018
[27] Ashburner J. A fast diffeomorphic image registration algorithm. NeuroImage. 2007; 38: 95–113. https://doi.org/10.1016/j.neuroimage.2007.07.007
[28] Goto M, Abe O, Aoki S, Hayashi N, Miyati T, Takao H, et al. Diffeomorphic Anatomical Registration Through Exponentiated Lie Algebra provides reduced effect of scanner for cortex volumetry with atlas-based method in healthy subjects. Neuroradiology. 2013; 55: 869–875. https://doi.org/10.1007/s00234-013-1193-2
[29] Whitwell JL. Voxel-based morphometry: an automated technique for assessing structural changes in the brain. The Journal of Neuroscience : the Official Journal of the Society for Neuroscience. 2009; 29: 9661–9664. https://doi.org/10.1523/JNEUROSCI.2160-09.2009
[30] Zatorre RJ, Fields RD, Johansen-Berg H. Plasticity in gray and white: neuroimaging changes in brain structure during learning. Nature Neuroscience. 2012; 15: 528–536. https://doi.org/10.1038/nn.3045
[31] Gothe NP, Hayes JM, Temali C, Damoiseaux JS. Differences in Brain Structure and Function Among Yoga Practitioners and

Controls. Frontiers in Integrative Neuroscience. 2018; 12: 26. https://doi.org/10.3389/fnint.2018.00026
[32] Gotink RA, Vernooij MW, Ikram MA, Niessen WJ, Krestin GP, Hofman A, et al. Meditation and yoga practice are associated with smaller right amygdala volume: the Rotterdam study. Brain Imaging and Behavior. 2018; 12: 1631–1639. https://doi.org/10.1007/s11682-018-9826-z
[33] Hernández SE, Suero J, Barros A, González-Mora JL, Rubia K. Increased Grey Matter Associated with Long-Term Sahaja Yoga Meditation: A Voxel-Based Morphometry Study. PloS One. 2016; 11: e0150757. https://doi.org/10.1371/journal.pone.0150757
[34] Villemure C, Ceko M, Cotton VA, Bushnell MC. Insular cortex mediates increased pain tolerance in yoga practitioners. Cerebral Cortex (New York, N.Y. : 1991). 2014; 24: 2732–2740. https://doi.org/10.1093/cercor/bht124
[35] Maric V, Ramanathan D, Mishra J. Respiratory regulation & interactions with neuro-cognitive circuitry. Neuroscience and Biobehavioral Reviews. 2020; 112: 95–106. https://doi.org/10.1016/j.neubiorev.2020.02.001
[36] Bleich M, Draguhn A, Ehmke H, Singer D. Physiologie, 10., Vollständig überarbeitete Auflage. Georg Thieme Verlag: Stuttgart New York. 2023.
[37] Barnett WH, Abdala AP, Paton JFR, Rybak IA, Zoccal DB, Molkov YI. Chemoreception and neuroplasticity in respiratory circuits. Experimental Neurology. 2017; 287: 153–164. https://doi.org/10.1016/j.expneurol.2016.05.036
[38] Fuller DD, Mitchell GS. Respiratory neuroplasticity - Overview, significance and future directions. Experimental Neurology. 2017; 287: 144–152. https://doi.org/10.1016/j.expneurol.2016.05.022
[39] Critchley HD, Nicotra A, Chiesa PA, Nagai Y, Gray MA, Minati L, et al. Slow breathing and hypoxic challenge: cardiorespiratory consequences and their central neural substrates. PloS One. 2015; 10: e0127082. https://doi.org/10.1371/journal.pone.0127082
[40] Bernardi L, Gabutti A, Porta C, Spicuzza L. Slow breathing reduces chemoreflex response to hypoxia and hypercapnia, and increases baroreflex sensitivity. Journal of Hypertension. 2001; 19: 2221–2229. https://doi.org/10.1097/00004872-200112000-00016
[41] Radaelli A, Raco R, Perfetti P, Viola A, Azzellino A, Signorini MG, et al. Effects of slow, controlled breathing on baroreceptor control of heart rate and blood pressure in healthy men. Journal of Hypertension. 2004; 22: 1361–1370. https://doi.org/10.1097/01.hjh.0000125446.28861.51
[42] Pramanik T, Sharma HO, Mishra S, Mishra A, Prajapati R, Singh S. Immediate effect of slow pace bhastrika pranayama on blood pressure and heart rate. Journal of Alternative and Complementary Medicine (New York, N.Y.). 2009; 15: 293–295. https://doi.org/10.1089/acm.2008.0440
[43] Russo MA, Santarelli DM, O'Rourke D. The physiological effects of slow breathing in the healthy human. Breathe (Sheffield, England). 2017; 13: 298–309. https://doi.org/10.1183/20734735.009817
[44] Juventin M, Ghibaudo V, Granget J, Amat C, Courtiol E, Buonviso N. Respiratory influence on brain dynamics: the preponderant role of the nasal pathway and deep slow regime. Pflugers Archiv : European Journal of Physiology. 2023; 475: 23–35. https://doi.org/10.1007/s00424-022-02722-7
[45] Lin IM, Tai LY, Fan SY. Breathing at a rate of 5.5 breaths per minute with equal inhalation-to-exhalation ratio increases heart rate variability. International Journal of Psychophysiology : Official Journal of the International Organization of Psychophysiology. 2014; 91: 206–211. https://doi.org/10.1016/j.ijpsycho.2013.12.006
[46] Modesti PA, Ferrari A, Bazzini C, Boddi M. Time sequence of autonomic changes induced by daily slow-breathing sessions. Clinical Autonomic Research : Official Journal of the Clinical Autonomic Research Society. 2015; 25: 95–104. https://doi.org/10.1007/s10286-014-0255-9
[47] Sharma VK, Trakroo M, Subramaniam V, Rajajeyakumar M, Bhavanani AB, Sahai A. Effect of fast and slow pranayama on perceived stress and cardiovascular parameters in young health-care students. International Journal of Yoga. 2013; 6: 104–110. https://doi.org/10.4103/0973-6131.113400
[48] Van Diest I, Verstappen K, Aubert AE, Widjaja D, Vansteenwegen D, Vlemincx E. Inhalation/Exhalation ratio modulates the effect of slow breathing on heart rate variability and relaxation. Applied Psychophysiology and Biofeedback. 2014; 39: 171–180. https://doi.org/10.1007/s10484-014-9253-x
[49] Yuenyongchaiwat K, Changsri K, Harnmanop S, Namdaeng P, Aiemthaisong M, Pongpanit K, et al. Effects of slow breathing training on hemodynamic changes, cardiac autonomic function and neuroendocrine response in people with high blood pressure: A randomized control trial. Journal of Bodywork and Movement Therapies. 2024; 37: 136–141. https://doi.org/10.1016/j.jbmt.2023.11.042
[50] Pal GK, Velkumary S, Madanmohan. Effect of short-term practice of breathing exercises on autonomic functions in normal human volunteers. The Indian Journal of Medical Research. 2004; 120: 115–121.
[51] Malhotra V, Javed D, Wakode S, Bharshankar R, Soni N, Porter PK. Study of immediate neurological and autonomic changes during *kapalbhati pranayama* in yoga practitioners. Journal of Family Medicine and Primary Care. 2022; 11: 720–727. https://doi.org/10.4103/jfmpc.jfmpc_1662_21
[52] Nayak R, Prakash S, Yadav RK, Upadhyay-Dhungel K. Kapalbhati changes cardiovascular parameters. Janaki Medical College Journal of Medical Science. 2016; 3: 43–49. https://doi.org/10.3126/jmcjms.v3i2.16080
[53] Lalitha S, Maheshkumar K, Shobana R, Deepika C. Immediate effect of *Kapalbhathi pranayama* on short term heart rate variability (HRV) in healthy volunteers. Journal of Complementary & Integrative Medicine. 2020; 18: 155–158. https://doi.org/10.1515/jcim-2019-0331
[54] Suzuki M, Tanuma T. The effect of nasal and oral breathing on airway collapsibility in patients with obstructive sleep apnea: Computational fluid dynamics analyses. PloS One. 2020; 15: e0231262. https://doi.org/10.1371/journal.pone.0231262
[55] Afzal M, Livesey A, Hameed MA, Mukherjee R. Obstructive sleep apnoea and hypertension: Current understanding, diagnosis and management. Clinical Medicine (London, England). 2026; 26: 100575. https://doi.org/10.1016/j.clinme.2026.100575
[56] Kalaskar R, Bhaje P, Kalaskar A, Faye A. Sleep Difficulties and Symptoms of Attention-deficit Hyperactivity Disorder in Children with Mouth Breathing. International Journal of Clinical Pediatric Dentistry. 2021; 14: 604–609. https://doi.org/10.5005/jp-journals-10005-1987
[57] May A. Experience-dependent structural plasticity in the adult human brain. Trends in Cognitive Sciences. 2011; 15: 475–482. https://doi.org/10.1016/j.tics.2011.08.002
[58] Shi HJ, Wang S, Wang XP, Zhang RX, Zhu LJ. Hippocampus: Molecular, Cellular, and Circuit Features in Anxiety. Neuroscience Bulletin. 2023; 39: 1009–1026. https://doi.org/10.1007/s12264-023-01020-1
[59] Villemure C, Čeko M, Cotton VA, Bushnell MC. Neuroprotective effects of yoga practice: age-, experience-, and frequency-dependent plasticity. Frontiers in Human Neuroscience. 2015; 9: 281. https://doi.org/10.3389/fnhum.2015.00281
[60] Hölzel BK, Carmody J, Vangel M, Congleton C, Yerramsetti

SM, Gard T, et al. Mindfulness practice leads to increases in regional brain gray matter density. Psychiatry Research. 2011; 191: 36–43. https://doi.org/10.1016/j.pscychresns.2010.08.006
[61] Garrison KA, Scheinost D, Constable RT, Brewer JA. BOLD signal and functional connectivity associated with loving kindness meditation. Brain and Behavior. 2014; 4: 337–347. https://doi.org/10.1002/brb3.219
[62] Dalton MA, D'Souza A, Lv J, Calamante F. New insights into anatomical connectivity along the anterior-posterior axis of the human hippocampus using *in vivo* quantitative fibre tracking. elife. 2022; 11: e76143. https://doi.org/10.7554/eLife.76143
[63] Grady CL. Meta-analytic and functional connectivity evidence from functional magnetic resonance imaging for an anterior to posterior gradient of function along the hippocampal axis. Hippocampus. 2020; 30: 456–471. https://doi.org/10.1002/hipo.23164
[64] Zheng Y, Tao S, Liu Y, Liu J, Sun L, Zheng Y, et al. Basal Forebrain-Dorsal Hippocampus Cholinergic Circuit Regulates Olfactory Associative Learning. International Journal of Molecular Sciences. 2022; 23: 8472. https://doi.org/10.3390/ijms23158472
[65] Zaccaro A, Piarulli A, Melosini L, Menicucci D, Gemignani A. Neural Correlates of Non-ordinary States of Consciousness in Pranayama Practitioners: The Role of Slow Nasal Breathing. Frontiers in Systems Neuroscience. 2022; 16: 803904. https://doi.org/10.3389/fnsys.2022.803904
[66] Allen HN, Bobnar HJ, Kolber BJ. Left and right hemispheric lateralization of the amygdala in pain. Progress in Neurobiology. 2021; 196: 101891. https://doi.org/10.1016/j.pneurobio.2020.101891
[67] von Leupoldt A, Sommer T, Kegat S, Baumann HJ, Klose H, Dahme B, et al. Dyspnea and pain share emotion-related brain network. NeuroImage. 2009; 48: 200–206. https://doi.org/10.1016/j.neuroimage.2009.06.015
[68] Stoeckel MC, Esser RW, Gamer M, von Leupoldt A. Breathlessness amplifies amygdala responses during affective processing. Psychophysiology. 2018; 55: e13092. https://doi.org/10.1111/psyp.13092
[69] Feinstein JS, Gould D, Khalsa SS. Amygdala-driven apnea and the chemoreceptive origin of anxiety. Biological Psychology. 2022; 170: 108305. https://doi.org/10.1016/j.biopsycho.2022.108305
[70] Vogt BA. Cingulate cortex in the three limbic subsystems. Handbook of Clinical Neurology. 2019; 166: 39–51. https://doi.org/10.1016/B978-0-444-64196-0.00003-0
[71] Smith R, Ahern GL, Lane RD. The role of anterior and midcingulate cortex in emotional awareness: A domain-general processing perspective. Handbook of Clinical Neurology. 2019; 166: 89–101. https://doi.org/10.1016/B978-0-444-64196-0.00006-6
[72] Fanselow MS, Dong HW. Are the dorsal and ventral hippocampus functionally distinct structures? Neuron. 2010; 65: 7–19. https://doi.org/10.1016/j.neuron.2009.11.031
[73] Nakamura NH, Oku Y, Fukunaga M. "Brain-breath" interactions: respiration-timing-dependent impact on functional brain networks and beyond. Reviews in the Neurosciences. 2023; 35: 165–182. https://doi.org/10.1515/revneuro-2023-0062
[74] Shouman K, Benarroch EE. Central Autonomic Network. In Chokroverty S, Cortelli P (eds.) Autonomic Nervous System and Sleep (pp. 9–18). Springer International Publishing: Cham. 2021. https://doi.org/10.1007/978-3-030-62263-3_2
[75] Belleau EL, Treadway MT, Pizzagalli DA. The Impact of Stress and Major Depressive Disorder on Hippocampal and Medial Prefrontal Cortex Morphology. Biological Psychiatry. 2019; 85: 443–453. https://doi.org/10.1016/j.biopsych.2018.09.031
[76] McKlveen JM, Myers B, Herman JP. The medial prefrontal cortex: coordinator of autonomic, neuroendocrine and behavioural responses to stress. Journal of Neuroendocrinology. 2015; 27: 446–456. https://doi.org/10.1111/jne.12272
[77] Jacobson L, Sapolsky R. The role of the hippocampus in feedback regulation of the hypothalamic-pituitary-adrenocortical axis. Endocrine Reviews. 1991; 12: 118–134. https://doi.org/10.1210/edrv-12-2-118
[78] Wingenfeld K, Wolf OT. Stress, memory, and the hippocampus. Frontiers of Neurology and Neuroscience. 2014; 34: 109–120. https://doi.org/10.1159/000356423
[79] Ortiz JB, Conrad CD. The impact from the aftermath of chronic stress on hippocampal structure and function: Is there a recovery? Frontiers in Neuroendocrinology. 2018; 49: 114–123. https://doi.org/10.1016/j.yfrne.2018.02.005
[80] Oparil S, Schmieder RE. New approaches in the treatment of hypertension. Circulation Research. 2015; 116: 1074–1095. https://doi.org/10.1161/CIRCRESAHA.116.303603
[81] Dampney RAL. Central neural control of the cardiovascular system: current perspectives. Advances in Physiology Education. 2016; 40: 283–296. https://doi.org/10.1152/advan.00027.2016
[82] Fang S, Zhang W. Heart-Brain Axis: A Narrative Review of the Interaction between Depression and Arrhythmia. Biomedicines. 2024; 12: 1719. https://doi.org/10.3390/biomedicines12081719
[83] Shoemaker JK, Goswami R. Forebrain neurocircuitry associated with human reflex cardiovascular control. Frontiers in Physiology. 2015; 6: 240. https://doi.org/10.3389/fphys.2015.00240
[84] Mah L, Szabuniewicz C, Fiocco AJ. Can anxiety damage the brain? Current Opinion in Psychiatry. 2016; 29: 56–63. https://doi.org/10.1097/YCO.0000000000000223
[85] Yoon SH, Song WS, Chung G, Kim SJ, Kim MH. Activity in the dorsal hippocampus-mPFC circuit modulates stress-coping strategies during inescapable stress. Experimental & Molecular Medicine. 2024; 56: 1921–1935. https://doi.org/10.1038/s12276-024-01294-z
[86] Salimi M, Javadi AH, Nazari M, Bamdad S, Tabasi F, Parsazadegan T, et al. Nasal Air Puff Promotes Default Mode Network Activity in Mechanically Ventilated Comatose Patients: A Noninvasive Brain Stimulation Approach. Neuromodulation : Journal of the International Neuromodulation Society. 2022; 25: 1351–1363. https://doi.org/10.1016/j.neurom.2021.11.003
[87] Zelano C, Jiang H, Zhou G, Arora N, Schuele S, Rosenow J, et al. Nasal Respiration Entrains Human Limbic Oscillations and Modulates Cognitive Function. The Journal of Neuroscience : the Official Journal of the Society for Neuroscience. 2016; 36: 12448–12467. https://doi.org/10.1523/JNEUROSCI.2586-16.2016
[88] Chaudhary IS, Shyi GCW, Huang STT. A systematic review and activation likelihood estimation meta-analysis of fMRI studies on arousing or wake-promoting effects in Buddhist meditation. Frontiers in Psychology. 2023; 14: 1136983. https://doi.org/10.3389/fpsyg.2023.1136983
[89] De Falco E, Solcà M, Bernasconi F, Babo-Rebelo M, Young N, Sammartino F, et al. Single neurons in the thalamus and subthalamic nucleus process cardiac and respiratory signals in humans. Proceedings of the National Academy of Sciences of the United States of America. 2024; 121: e2316365121. https://doi.org/10.1073/pnas.2316365121
[90] Chang DG, Holt JA, Sklar M, Groessl EJ. Yoga as a treatment for chronic low back pain: A systematic review of the literature. Journal of Orthopedics & Rheumatology. 2016; 3: 1–8.
[91] Cramer H, Lauche R, Anheyer D, Pilkington K, de Manincor M, Dobos G, et al. Yoga for anxiety: A systematic review and meta-analysis of randomized controlled trials. Depression and Anxiety. 2018; 35: 830–843. https://doi.org/10.1002/da.22762
[92] Falkenberg RI, Eising C, Peters ML. Yoga and immune system functioning: a systematic review of randomized controlled tri-

als. Journal of Behavioral Medicine. 2018; 41: 467–482. https://doi.org/10.1007/s10865-018-9914-y

[93] Slagter L, Demyttenaere K, Verschueren P, De Cock D. The Effect of Meditation, Mindfulness, and Yoga in Patients with Rheumatoid Arthritis. Journal of Personalized Medicine. 2022; 12: 1905. https://doi.org/10.3390/jpm12111905

[94] Ye X, Chen Z, Shen Z, Chen G, Xu X. Yoga for Treating Rheumatoid Arthritis: A Systematic Review and Meta-Analysis. Frontiers in Medicine. 2020; 7: 586665. https://doi.org/10.3389/fmed.2020.586665

[95] Ulloa Severino FP, Lawal OO, Sakers K, Wang S, Kim N, Friedman AD, et al. Training-induced circuit-specific excitatory synaptogenesis in mice is required for effort control. Nature Communications. 2023; 14: 5522. https://doi.org/10.1038/s41467-023-41078-z

[96] Chen L, Li Z, Wang W, Zhou Y, Li W, Wang Y. Adult hippocampal neurogenesis: New avenues for treatment of brain disorders. Stem Cell Reports. 2025; 20: 102600. https://doi.org/10.1016/j.stemcr.2025.102600